



Leaf-scale quantification of the effect of photosynthetic gas exchange on $\Delta^{17}\text{O}$ of atmospheric CO_2

Getachew Agmuas Adnew¹, Thijs L. Pons², Gerbrand Koren³, Wouter Peters^{3,4}, Thomas Röckmann¹

¹Institute for Marine and Atmospheric research Utrecht (IMAU), Utrecht University, The Netherlands

5 ²Institute of Environmental Biology, Utrecht University, The Netherlands

³Department of Meteorology and Air Quality, Wageningen University, The Netherlands

⁴Centre for Isotope Research, University of Groningen, The Netherlands

Correspondence to: Getachew Agmuas Adnew (getachewagmuas@gmail.com)

10

Abstract

15

20

25

Understanding the processes that affect the triple oxygen isotope composition of atmospheric CO_2 during gas exchange can help constrain the interaction and fluxes between the atmosphere and the biosphere. We conducted leaf cuvette experiments under controlled conditions, using three plant species. The experiments were conducted at two different light intensities and using CO_2 with different ^{17}O -excess. The oxygen isotope composition of CO_2 was used to estimate c_m , the mole fraction of CO_2 at the CO_2 - H_2O exchange site. Our results demonstrate that two key factors determine the effect of gas exchange on the $\Delta^{17}\text{O}$ of atmospheric CO_2 . The relative difference between $\Delta^{17}\text{O}$ of the CO_2 entering the leaf and the CO_2 in equilibrium with leaf water, and the back-diffusion flux of CO_2 from the leaf to the atmosphere, which can be quantified by the c_m/c_a ratio where c_a is the CO_2 mole fraction in the surrounding air. At low c_m/c_a ratio the discrimination is governed mainly by diffusion into the leaf, and at high c_m/c_a ratio by back-diffusion of CO_2 that has equilibrated with the leaf water. Plants with a higher c_m/c_a ratio modify the $\Delta^{17}\text{O}$ of atmospheric CO_2 more strongly than plants with a lower c_m/c_a ratio. Based on the leaf cuvette experiments, the global value for discrimination against $\Delta^{17}\text{O}$ of atmospheric CO_2 during the photosynthetic gas exchange is estimated to be $-0.57 \pm 0.14\text{‰}$ using c_m/c_a values of 0.3 and 0.7 for C_4 and C_3 plants, respectively. The main uncertainties in this global estimate arise from variation in c_m/c_a ratios among plants and growth conditions.

30

1. Introduction

35

Stable isotope measurements of CO_2 provide important information on the magnitude of the CO_2 fluxes between atmosphere and biosphere, which are the largest components of the global carbon cycle (Farquhar et al., 1989a;1993;Ciais et al., 1997a;1997b;Flanagan and Ehleringer, 1998;Yakir and Sternberg, 2000;Gillon and Yakir, 2001;Cuntz et al., 2003a;2003b). A better understanding of the terrestrial carbon cycle is essential for predicting future climate and atmospheric CO_2 mole fractions (Booth et al., 2012). Gross primary productivity (GPP), the total carbon dioxide uptake by vegetation during photosynthesis, can only be determined indirectly and remains poorly constrained (Cuntz, 2011;Welp et al., 2011). For example, Beer et al. (2010) estimated global GPP to be 102-135 PgC yr^{-1}



- 40 (85% confidence interval, CI) using machine learning techniques by extrapolating from a database of eddy-covariance measurements of CO₂ fluxes. This estimate has since then been widely used as target for terrestrial vegetation models (Sitch et al., 2015), and replicated using extensions on the technique (Jung et al., 2019). As an alternative, (Welp et al., 2011) estimated global GPP to be 150-175 PgC yr⁻¹ using variations in δ¹⁸O of atmospheric CO₂ after El Nino events.
- 45 The concept behind the latter study was that atmospheric CO₂ exchanges oxygen isotopes with leaf and soil water, and this isotope exchange mostly determines the observed variations in δ¹⁸O of CO₂ (Francey and Tans, 1987; Yakir, 1998); see below for definition of the delta value. Following the 97/98 ENSO event, the anomalous δ¹⁸O signature imposed on tropical leaf and soil waters was transferred to atmospheric CO₂, before slowly disappearing as a function of the lifetime of atmospheric CO₂. This in turn is governed by the land vegetation uptake of CO₂ during photosynthesis, as well as soil invasion of CO₂ (Miller et al., 1999; Wingate et al., 2009). In addition to the latter term, the equilibration of CO₂ with water is an uncertain parameter in this calculation, partly because the δ¹⁸O of water at the site of isotope exchange in the leaf is not well defined. Importantly, a significant but variable δ¹⁸O gradient can occur in leaves due to the preferential evaporation of H₂¹⁶O relative to H₂¹⁸O (Gan et al., 2002; Farquhar and Gan, 2003; Gan et al., 2003; Cernusak et al., 2016), which induces a considerable uncertainty in estimating δ¹⁸O of the isotopically exchanged CO₂. Similar considerations for the transfer of the δ¹⁸O signature of precipitation into the soils, and then up through the roots, stems, and leaves make ¹⁸O of CO₂ a challenging measurement to interpret (Cuntz et al., 2003a; 2003b; Peylin et al., 1999).
- 50
- 55
- 60 The ¹⁷O-excess of CO₂ (Δ¹⁷O, involving the triple oxygen isotope composition of CO₂, see equation 5) has been suggested as additional independent tracer for constraining global GPP (Hoag et al., 2005; Thiemens et al., 2013; Hofmann et al., 2017; Liang et al., 2017b; Koren et al., 2019). Because Δ¹⁷O is not or only slightly sensitive to mass-dependent fractionation processes acting on CO₂ and H₂O, its interpretation may be less sensitive to the effects mentioned above. In the stratosphere, CO₂ obtains a considerable ¹⁷O-excess due to the transfer of oxygen atoms from ¹⁷O-enriched ozone to CO₂ via photochemical isotope exchange (Thiemens et al., 1991; 1995; Lyons, 2001; Lämmerzahl et al., 2002; Thiemens, 2006; Kawagucci et al., 2008). Once this anomalous signature has been created in the stratosphere, the only process that removes the anomaly is isotope exchange with leaf water, soil water and ocean water at the Earth's surface, after CO₂ has re-entered the troposphere (Boering, 2004; Thiemens et al., 2014; Liang and Mahata, 2015; Hofmann et al., 2017). Isotope exchange with water in clouds and rain droplets is negligible due to the absence of carbonic anhydrase (Francey and Tans, 1987).
- 65
- 70

Isotope exchange with leaf water is more efficient relative to ocean water due to the presence of the enzyme carbonic anhydrase (CA), which effectively catalyzes the conversion of CO₂ and H₂O to HCO₃⁻ and H⁺ and vice versa (Francey and Tans, 1987; Friedli et al., 1987; Badger and Price, 1994; Gillon and Yakir, 2001). Therefore, CO₂ quickly equilibrates its isotopic composition with that of leaf water with a well-established temperature dependent fractionation factor (Brenninkmeijer et al., 1983; Barkan and Luz, 2012). The ¹⁷O-excess of CO₂ (Δ¹⁷O) (equation 4) at the CO₂-H₂O exchange site in the leaf will vary much less than δ¹⁸O because the transfer of water from the precipitation to the leaves, as well as

75



80 evaporation, are mass dependent processes with a well-known three isotope slope (Barkan and Luz, 2005; Landais et al., 2006). Therefore, $\Delta^{17}\text{O}$ may be a more robust tracer for GPP than $\delta^{18}\text{O}$ (Hoag et al., 2005; Hofmann et al., 2017; Koren et al., 2019).

85 Several measurements of $\Delta^{17}\text{O}$ of CO_2 in atmospheric samples from different locations have been performed to use it as a tracer for GPP (Liang et al., 2006; Barkan and Luz, 2012; Thiemens et al., 2014; Liang and Mahata, 2015; Laskar et al., 2016; Hofmann et al., 2017; Liang et al., 2017b). A significant limitation of such studies is that the triple oxygen isotope signatures associated with the large CO_2 exchange fluxes (photosynthesis, respiration, soil invasion) are not well established, and in many cases are based on assumptions, but not confirmed by measurement (Koren et al., 2019). Further interpretation
90 of $\Delta^{17}\text{O}$ measurements depends on our ability to understand and untangle the individual processes.

The effect of vegetation on the isotope composition of atmospheric CO_2 depends on the type of plant metabolism. Generally, plants are classified as C_3 and C_4 based on their metabolism. For detail explanation about the type of plants the reader is directed to (Ehleringer and Monson, 1993; Ehleringer and Cerling, 2002; Ubierna et al., 2018; Ubierna et al., 2019; Cousins et al., 2020). In C_3 plants, the CO_2 diffuses through the boundary layer surrounding the leaf, the stomata, the intercellular air space, cell wall, plasma membrane, cytosol, chloroplast envelope and stroma where it is carboxylated into C_3 acid by Ribulose-1,5-bisphosphate carboxylase oxygenase RubisCO (Farquhar et al., 1982; Evans et al., 2009; Ubierna et al., 2019; Cousins et al., 2020) (Figure 1). For C_4 plants, CO_2 is initially carboxylated
100 into C_4 acid by phosphoenolpyruvate carboxylase (PEPC) in the mesophyll cytosol (Sage and Monson, 1998; Caemmerer et al., 2014; Cousins et al., 2020) (Figure 1). The mole fraction of CO_2 at the CO_2 - H_2O exchange site (c_m) is an important parameter to determine the effect of photosynthesis on the triple oxygen isotope composition of atmospheric CO_2 . In C_3 plants, CA is found in the chloroplast, cytosol, mitochondria and plasma membrane (Fabre et al., 2007; DiMario et al., 2016), the CO_2 - H_2O exchange can
105 occur anywhere between the plasma membrane and within the chloroplast. For C_4 plants, CA is mainly found in the cytosol, the CO_2 - H_2O exchange occurs in the cytosol (Badger and Price, 1994).

In this study we report the effect of photosynthesis on the $\Delta^{17}\text{O}$ of CO_2 in the surrounding air at the leaf level, using three species that are representative for three different biomes. The fast-growing annual herbaceous C_3 species *Helianthus annuus* (sunflower) has a high photosynthetic capacity (A_{max}) and high stomatal conductance (g_s) and is representative for temperate and tropical crops (Fredeen et al., 1991). The slower growing perennial evergreen C_3 species *Hedera hybernica* (ivy) is representative of forests and other woody vegetation and stress subjected habitats (Pons et al., 2009). The fast-growing, agronomically important crop *Zea mays* (maize) is an herbaceous annual C_4 species with a high A_{max} and
115 a low g_s , typical for savanna type vegetation (Weijde et al., 2013). Sunflower and ivy are used to cover the c_m/c_a ratio among C_3 plants and maize represents c_m/c_a ratio for the C_4 plants. We measured the triple oxygen isotopic composition of CO_2 entering and leaving the leaf cuvette to calculate the isotopic fractionation associated with photosynthesis. Using these results, we estimated the effect of terrestrial vegetation on $\Delta^{17}\text{O}$ of CO_2 in the global atmosphere.

120



2. Theory

2.1. Notation and definition of δ values

Isotopic composition is expressed as the relative deviation of the heavy to light isotope ratio in a sample relative to reference material and it is denoted as δ (McKinney et al., 1950), expressed in per mill (‰).

125 In the case of oxygen isotopes, the deviation of the two isotope ratios $^{18}\text{R} = [^{18}\text{O}]/[^{16}\text{O}]$ and $^{17}\text{R} = [^{17}\text{O}]/[^{16}\text{O}]$ from an international reference ratio (Vienna Standard Mean Ocean Water, VSMOW) is quantified in δ notation as:

$$\delta^{18}\text{O} = \frac{^{18}\text{R}_{\text{sample}}}{^{18}\text{R}_{\text{VSMOW}}} - 1 \quad (1)$$

$$\delta^{17}\text{O} = \frac{^{17}\text{R}_{\text{sample}}}{^{17}\text{R}_{\text{VSMOW}}} - 1 \quad (2)$$

130

For most processes, isotope fractionation depends on mass, and therefore the fractionation against ^{17}O is approximately half of the fractionation against ^{18}O (equation 3).

$$\ln(\delta^{17}\text{O} + 1) = \lambda \times \ln(\delta^{18}\text{O} + 1) \quad (3)$$

135 The factor λ ranges from 0.5 to 0.5305 for different molecules and process (Matsuhisa et al., 1978; Young et al., 2002; Thiemens, 1999; Cao and Liu, 2011). This relation is generally referred to as mass dependent fractionation and can also be expressed as $\left[\frac{^{17}\text{R}}{^{17}\text{R}_{\text{ref}}} = \left(\frac{^{18}\text{R}}{^{18}\text{R}_{\text{ref}}} \right)^\lambda \right]$ or $\alpha^{17} = (\alpha^{18})^\lambda$ where α^{17} and α^{18} are the fractionations of ^{17}O and ^{18}O relative to a reference material, respectively. For small δ^{17} and δ^{18} values, equation (3) can be linearized to $\delta^{17}\text{O} = \lambda \times \delta^{18}\text{O}$. $\Delta^{17}\text{O}$ is used to quantify the degree of deviation from equation (3) (see equation 4). Note that deviations from a chosen reference slope λ are not only caused
140 by mass independent fractionation process, but can also be introduced by mass dependent process with a different three isotope slope relative to the chosen reference line (Barkan and Luz, 2005; Landais et al., 2006; 2008; Luz and Barkan, 2010; Barkan and Luz, 2011; Pack and Herwartz, 2014).

$$\Delta^{17}\text{O} = \ln(\delta^{17}\text{O} + 1) - \lambda \times \ln(\delta^{18}\text{O} + 1) \quad (4)$$

145 The choice of λ is in principle arbitrary and in this study, we used $\lambda = 0.528$, the value associated with meteoric water (Meijer and Li, 1998; Landais et al., 2008; Brand et al., 2010; Luz and Barkan, 2010; Barkan and Luz, 2012; Sharp et al., 2018). Note that $\Delta^{17}\text{O}$ is not a measured quantity, it is inferred from measurements of $\delta^{17}\text{O}$ and $\delta^{18}\text{O}$.

150 2.2. Calculation of the discrimination in the oxygen isotope anomaly of CO_2



155 The overall isotope fractionation associated with the photosynthesis of CO₂ is commonly quantified using the term discrimination as described in (Farquhar and Richards, 1984; Farquhar et al., 1989a; Farquhar and Lloyd, 1993). We use the symbol Δ_A for discrimination due to assimilation in this manuscript since the commonly used Δ is already used for the definition of ¹⁷O-excess (see above). Δ_A quantifies the enrichment or depletion of carbon and oxygen isotopes of CO₂ in the surrounding atmosphere relative to the CO₂ that is assimilated (Farquhar and Richards, 1984). It can be calculated from the isotopic composition of the CO₂ entering and leaving the leaf cuvette (Evans et al., 1986; Gillon and Yakir, 2000b; Barbour et al., 2016), for instance for ¹⁸O-photosynthetic discrimination, as:

$$\Delta_A^{18}\text{O}_{\text{obs}} = \frac{{}^{18}\text{R}_a}{{}^{18}\text{R}_A} - 1 = \frac{\delta^{18}\text{O}_a - \delta^{18}\text{O}_A}{1 + \delta^{18}\text{O}_A} = \frac{\zeta \times (\delta^{18}\text{O}_a - \delta^{18}\text{O}_e)}{1 + \delta^{18}\text{O}_a - \zeta \times (\delta^{18}\text{O}_a - \delta^{18}\text{O}_e)} \quad (5)$$

160 where the indices *e*, *a* and *A* refer to CO₂ entering (*e*) and leaving (*a*) the cuvette and being assimilated (*A*), respectively. $\zeta = \frac{c_e}{c_e - c_a}$, where *c_e* and *c_a* are the mole fractions of CO₂ entering and leaving the leaf cuvette. The observed ¹⁷O-photosynthetic discrimination (Δ_A¹⁷O_{obs}) is calculated analogously. We note that the concept of discrimination associated with photosynthesis is more complicated for the oxygen isotopes compared to ¹³C. For ¹³C, the observed isotope change is directly associated with an isotope effect in assimilation due to RubisCO and PEPC. For the oxygen isotopes, the observed change in isotopic composition is caused by oxygen isotope exchange of CO₂ with leaf water rather than by fractionation in the assimilation process itself.

170 The discrimination against Δ¹⁷O associated with assimilation in global models, assuming the degree of equilibration between CO₂ and H₂O is unity, is calculated as shown in equation 6 (Hofmann et al., 2017; Liang et al., 2017b; Koren et al., 2019).

$$\Delta_A \Delta^{17}\text{O} = (\lambda_{\text{diffusion}} - \lambda_{RL}) \times \ln(\bar{a}_{18} + 1) + (\Delta^{17}\text{O}_m - \Delta^{17}\text{O}_a) \frac{c_m}{c_a - c_m} \quad (6)$$

175 \bar{a}_{18} , is the weighted mean of discrimination occurring during the diffusion of ¹²C¹⁸O¹⁶O from the ambient air to the CO₂-H₂O exchange site and it is estimated to be 7.4‰ (Farquhar et al., 1993). This value has been adopted in several global studies of δ¹⁸O of atmospheric CO₂ (Ciais et al., 1997a; 1997b; Cuntz et al., 2003a; 2003b) and the global Δ¹⁷O studies (Hofmann et al., 2017; Liang et al., 2017b; Koren et al., 2019). $\lambda_{\text{diffusion}} = 0.509$ is the coefficient associated the fractionation of C¹⁷OO as it diffuses through air relative to C¹⁸OO (Young et al., 2002) and $\lambda_{RL} = 0.528$ (the reference slope used in this study). Δ¹⁷O_m and *c_m* are the oxygen isotope anomaly and mole fraction of CO₂ at the CO₂-H₂O exchange site, respectively.

185 A good approximation for the observed ¹⁸O-discrimination can be derived from the leaf exchange parameters (Farquhar and Lloyd, 1993), see supplementary material for the derivation, as:



$$\Delta_A^{18}O_{FM} = \frac{\bar{a}_{18} + \frac{c_m}{c_a - c_m} \times \delta^{18}O_{ma}}{1 - \frac{c_m}{c_a - c_m} \times \delta^{18}O_{ma}} \approx \bar{a}_{18} + \frac{c_m}{c_a - c_m} \times (\delta^{18}O_m - \delta^{18}O_a) \quad (7)$$

The subscript *FM* stands for Farquhar model. $\delta^{18}O_{ma}$ is the enrichment in $\delta^{18}O$ of CO_2 in full isotopic equilibrium with water at the exchange site relative to the CO_2 in the surrounding air. $\delta^{18}O_{ma}$ is calculated as:

$$\delta^{18}O_{ma} = \frac{\delta^{18}O_m - \delta^{18}O_a}{1 + \delta^{18}O_a} \quad (8)$$

190 $\delta^{18}O_m$ is the isotope composition of CO_2 in equilibrium with leaf water at the CO_2 - H_2O exchange site (equation 16). Analogous to $\Delta_A^{18}O_{FM}$, a similar equation for $\Delta_A^{17}O_{FM}$ can be derived like equation 7 (see equation S12, supplementary material). In the global models (Hofmann et al., 2017; Liang et al., 2017b; Koren et al., 2019), $\Delta^{17}O$ -photosynthetic discrimination shown in equation 6 is derived from $\Delta_A^{17}O_{FM}$ and $\Delta_A^{18}O_{FM}$ as shown from equation 9 to 11.

$$\Delta_A \Delta^{17}O = \left(\bar{a}_{17} + \frac{c_m}{c_a - c_m} (\delta^{17}O_m - \delta^{17}O_a) \right) - \lambda_{RL} \times \left(\bar{a}_{18} + \frac{c_m}{c_a - c_m} (\delta^{18}O_m - \delta^{18}O_a) \right) \quad (9)$$

195

$$\Delta_A \Delta^{17}O = (\bar{a}_{17} - \lambda_{RL} \times \bar{a}_{18}) + [(\delta^{17}O_m - \lambda_{RL} \delta^{18}O_m) - (\delta^{17}O_a - \lambda_{RL} \delta^{18}O_a)] \frac{c_m}{c_a - c_m} \quad (10)$$

$$\Delta_A \Delta^{17}O = (\bar{a}_{17} - \lambda_{RL} \times \bar{a}_{18}) + [\Delta^{17}O_m - \Delta^{17}O_a] \frac{c_m}{c_a - c_m} \quad (11)$$

200 Note that, $\ln(\bar{a}_{18} + 1) \approx \bar{a}_{18}$ and $(\bar{a}_{17} - \lambda_{RL} \times \bar{a}_{18}) = (\lambda_{diffusion} - \lambda_{RL}) \times \ln(\bar{a}_{18} + 1)$, i.e. the left and right side of equation 11 is similar to the left and right side of equation 6, respectively. For the leaf cuvette experiments, the $\Delta_A \Delta^{17}O$ is calculated with $\lambda_{RL} = 0.528$ as:

$$\Delta_A \Delta^{17}O_{obs} = \ln(\Delta_A^{17}O_{obs} + 1) - 0.528 \times \ln(\Delta_A^{18}O_{obs} + 1) \quad (12)$$

205 $\Delta^{17}O$ calculated using equation 4 (logarithmic definition) is not a conserved quantity. Adding or subtracting $\Delta^{17}O$ results calculated using equation 4 (logarithmic definition) results in an error that gets larger when the relative difference in $\delta^{18}O$ between the two CO_2 gases increases regardless of the $\Delta^{17}O$ of the individual CO_2 gases (Figure 1). The discrepancy of adding and subtracting $\Delta^{17}O$ with a logarithmic definition is the largest when the two CO_2 gases are mixed in equal proportions (50:50). To avoid this error either the subtraction and addition should be done in small δ 's (see below) and $\Delta^{17}O$ value should



210 be calculated from the small δ 's differences or use the linear definition of the anomaly ($\Delta^{17}\text{O} = \delta^{17}\text{O} - \lambda \times \delta^{18}\text{O}$) (Liang et al., 2017b). (Liang et al., 2017b), in their global mass balance budget calculation, reported adding and subtracting the anomaly with logarithmic definition results in a 10% error in each reservoir.

215 2.3. Isoflux calculation for $\Delta_A\Delta^{17}\text{O}$

An isoflux is the product of isotope composition and gross mass flux of the molecule. In the case of assimilation, which is a net sink, the net flux $F_A = F_{AL} - F_{LA}$ is multiplied with the discrimination associated with assimilation. F_{LA} and F_{AL} are total CO_2 fluxes from leaf to the atmosphere and from atmosphere to leaf, respectively. The global $\Delta_A^{18}\text{O}$ -isoflux is $F_A \times \Delta_A^{18}\text{O}$ (Farquhar et al., 1993; Ciais et al., 1997a; 1997b; Gillon and Yakir, 2001; Cuntz et al., 2003a; 2003b).

The leaf scale discrimination against $\Delta^{17}\text{O}$ is then extrapolated to global vegetation using representative values for $\Delta_A\Delta^{17}\text{O}_{C4}$ and $\Delta_A\Delta^{17}\text{O}_{C3}$, considering the observed discriminations as a function of the c_m/c_a ratio and the global average values for $\Delta^{17}\text{O}$ of leaf water and atmospheric CO_2 , and the relative fractions of photosynthesis by C_4 and C_3 plants, respectively as:

$$\Delta_A\Delta^{17}\text{O}_{\text{global}} = f_{C4} \times \Delta_A\Delta^{17}\text{O}_{C4} + f_{C3} \times \Delta_A\Delta^{17}\text{O}_{C3} \quad (13)$$

where f_{C4} and f_{C3} are the photosynthesis weighted global coverage of C_4 and C_3 vegetation. $\Delta_A\Delta^{17}\text{O}_{C4}$ and $\Delta_A\Delta^{17}\text{O}_{C3}$ quantify the discrimination against $\Delta^{17}\text{O}$ by C_4 and C_3 plants, which are calculated using estimated values of c_m/c_a from a model. The global scale $\Delta^{17}\text{O}_A$ isoflux is calculated by multiplying the discrimination with the assimilation flux.

$$F_A \times \Delta_A\Delta^{17}\text{O} = A \times (f_{C4} \times \Delta_A\Delta^{17}\text{O}_{C4} + f_{C3} \times \Delta_A\Delta^{17}\text{O}_{C3}) \quad (14)$$

where, $A=0.88 \times \text{GPP}$ is the terrestrial assimilation rate, the factor 0.88 accounts for the fraction of CO_2 released due to autotrophic respiration (Ciais et al., 1997a).

235 2.4. Mole fraction of CO_2 at the site of $\text{CO}_2\text{-H}_2\text{O}$ exchange

Following (Farquhar and Cernusak, 2012; Barbour et al., 2016; Osborn et al., 2017), the CO_2 mole fraction at the site of $\text{CO}_2\text{-H}_2\text{O}$ exchange is calculated as:

$$c_m = c_i \left(\frac{\delta^{18}\text{O}_i - a_{18w} - \delta^{18}\text{O}_A \times (1 + a_{18w})}{\delta^{18}\text{O}_m - a_{18w} - \delta^{18}\text{O}_A \times (1 + a_{18w})} \right) \quad (15)$$

240 where $\delta^{18}\text{O}_i$ is $\delta^{18}\text{O}$ of CO_2 in the intercellular airspace (Farquhar and Cernusak, 2012), a_{18w} is the fractionation of $\delta^{18}\text{O}$ of CO_2 during diffusion and dissolution in water (0.8‰) (Farquhar and Lloyd, 1993),

$\delta^{18}\text{O}_A$ is $\delta^{18}\text{O}$ of the assimilated CO_2 and $\delta^{18}\text{O}_m$ is the $\delta^{18}\text{O}$ of CO_2 in equilibrium with leaf water at the CO_2 - H_2O exchange site. Assuming the isotopic composition of leaf water at the CO_2 - H_2O exchange site is the same as the $\delta^{18}\text{O}$ of leaf water at the evaporation site, $\delta^{18}\text{O}_m$ can be calculated as:

$$\delta^{18}\text{O}_m = (\delta^{18}\text{O}_{\text{wes}} + 1) \times (1 + \epsilon_w^{18}) - 1 \quad (16)$$

where $\delta^{18}\text{O}_{\text{wes}}$ is the $\delta^{18}\text{O}$ of H_2O at the exchange site and ϵ_w^{18} is the equilibrium fractionation between CO_2 and water (equation 18). The $\delta^{18}\text{O}_{\text{wes}}$ is calculated using the modified Craig and Gordon model (Farquhar et al., 1989b; Flanagan et al., 1991; Harwood et al., 1998) as:

$$\delta^{18}\text{O}_{\text{wes}} = \delta^{18}\text{O}_{\text{trans}} + \epsilon_k^{18} + \epsilon_{\text{equ}}^{18} + \frac{w_a}{w_i} \times (\delta^{18}\text{O}_{\text{wa}} - \epsilon_k^{18} + \delta^{18}\text{O}_{\text{trans}}) \quad (17)$$

where w_i and w_a are the mole fraction of water vapor inside the leaf and in the air leaving the cuvette and ϵ_k^{18} and $\epsilon_{\text{equ}}^{18}$ are the kinetic fractionation of water vapor in the air and the equilibrium fractionation between liquid and gas phase water, respectively (see Appendix 2). The equilibrium fractionation between CO_2 and water (ϵ_w^{18}) is temperature dependent and is calculated after (Brenninkmeijer et al., 1983) as:

$$\epsilon_w^{18} = \frac{17604}{T} - 17.93 \quad (18)$$

where T is leaf temperature. Analogous to $\delta^{18}\text{O}$, the mole fraction of CO_2 in the mesophyll cell can be calculated using $\delta^{17}\text{O}$ values (Appendix 3, equation A3.6). The detailed derivation for the c_m calculation is shown in appendix 3.

3. Materials and methods

3.1. Plant material and growth conditions

Sunflower (*Helianthus annuus* L. cv “sunny”) was grown from seeds in 0.6 L pots with potting soil (Primasta, the Netherlands). The dwarf type sunflowers were grown until the first leaf pair that was used for the experiments reached the final size, which is about 4 weeks. All leaves appearing above the first leaf pair were removed to avoid shading. Established juvenile Ivy (*Hedera hibernica* L.) plants were pruned and planted in 6 L pots. After at least 6 weeks in the growth chamber, leaves that had developed and matured there were used for the experiments. Mays (*Z. mays* L. cv “saccharate”) was grown from seed in 1.6 L pots for at least 7 weeks. The 4th or higher leaf number was used for the experiments when mature. A section of the leaf at about 1/3 from the tip was inserted in the leaf cuvette. The pots with the potting soil were soaked in a complete nutrient solution containing 6.6 mM nitrate (Millenaar et al., 2005) after planting and applied weekly during growth. They were placed on a sub-irrigation system that provided water during the growth period in a controlled environment growth chamber, air temperature 20°C, relative humidity 70% and CO_2 mole fraction of about 400 ppm. The photosynthetic photon flux density (PPFD) was about 300 $\mu\text{mol m}^{-2} \text{s}^{-1}$ during a daily photoperiod of 16 hours measured with a PPFD meter (Licor LI-250A, Li-Cor Inc, Nebraska, USA).



3.2. Gas exchange experiments

280 Gas exchange experiments were performed in an open system where a controlled flow of air enters and leaves the leaf cuvette similar to the setup used by (Pons and Welschen, 2002). A schematic of the gas exchange experimental setup is shown in Figure 2. The leaf cuvette had dimensions of 7 x 7 x 7 cm³ (lxwxh) and the top part of the cuvette was transparent. The temperature of the leaf was measured with a K type thermocouple. The leaf chamber temperature was controlled by a temperature-controlled water bath kept at 20°C (Tamson TLC 3, The Netherlands). A fan inside the chamber was used to mix the air inside the cuvette thoroughly and to create a high boundary layer conductance. A halogen lamp in a slide projector was used as a light source. Infrared was excluded by reflection from a cold mirror. The light intensity was varied by with spectrally neutral filters.

290 The CO₂ mole fraction of the incoming and outgoing air was measured with an infrared gas analyzer (IRGA, model LI-6262, LI-COR Inc., Nebraska, USA). The isotopic composition and mole fraction of the incoming and outgoing water vapor were measured with a triple water vapor isotope analyzer (WVIA, model 911-0034, Los Gatos Research, USA). Compressed air (ambient outside air without drying) was passed through soda lime to scrub the CO₂. The CO₂ free air could be humidified depending on the experiment conditions (see Figure 2). The humidity of the inlet air was monitored continuously with a dewpoint meter (General Eastern, Watertown, MA, USA). Pure CO₂ (either normal CO₂ or isotopically enriched CO₂) was mixed with the incoming air to produce a CO₂ mole fraction of 500 ppm. The isotopically enriched CO₂ was prepared by photochemical isotope exchange between CO₂ and O₂ under UV irradiation, as described in detail in (Adnew et al., 2019).

300 An attached leaf or part of it was inserted in the cuvette., the composition of the inlet air was measured, and both IRGA and WVIA were switched to measure the outlet air. Based on the CO₂ mole fraction of the outgoing air the flow rate of the incoming air to the cuvette was adjusted to establish a drawdown of 100 ppm CO₂ due to photosynthesis in the plant chamber. The vapor pressure of the water vapor entering the cuvette is adjusted to the transpiration rate relative to CO₂ uptake (Figure 2). The outgoing air was measured continuously until a steady state was reached for CO₂ and water mole fractions and δD and $\delta^{18}O$ of the water vapor. After a steady state was established, the air was directed to the sampling flask while the IGRA and WVIA were switched back to measure the inlet air. The air passed through a Mg(ClO₄)₂ dryer before entering the sampling flask.

310 After sampling, the leaf area inside the cuvette was measured with a LI-3100C area meter (Li-COR, Inc. USA). Immediately afterward, the leaf was placed in a leak tight 9 mL glass vial and kept in a freezer at -20°C until leaf water extraction.

3.3. Calibration of the Water Vapor Isotope Analyzer (WVIA)

315 The WVIA was calibrated using five water standards provided by IAEA (Wassenaar et al., 2018) for both $\delta^{18}O$ and δD . We did not calibrate the WVIA for $\delta^{17}O$, so the $\delta^{17}O$ data are not used in the quantitative



320 evaluation. The results are shown in supplementary material Figure S1. The isotopic composition of the
water standards ranged from -50.93 to 3.64‰ and -396.98 to 25.44‰ for δD and $\delta^{18}O$, respectively.
Based on the calibration using the five standards, a working standard was prepared to correct for short-
term variability and to determine the non-linearity (dependency of δD and $\delta^{18}O$ on the water vapor mole
fraction). Each day the LGR was calibrated with 3 standards that cover the isotopic composition of the
samples measured ($\delta^{18}O$ value of -24.777‰, -8.640‰ and 0.11‰, provided by IAEA (Wassenaar et al.,
2018)).

325 Supplementary Figure S2, shows the results of the non-linearity tests. All three isotope signatures of water
vapor showed relatively different dependence on the mole fraction of water vapor measured. The $\delta^{18}O$ is
independent of the mole fraction above 11000 ppm but decreases at lower mole fraction until 4000 ppm,
and then increases again. $\delta^{17}O$ is relatively stable for mole fractions higher than 17000 ppm, but increases
strongly and in a non-linear manner below. Similarly, δD is independent of the mole fraction of water
vapor above 10000 ppm but increases non-linearly below. $\delta^{18}O$, $\delta^{17}O$ and δD values measured with the
WVIS are dependent on the type of carrier gas used when measuring liquid samples as shown for pure
330 N_2 and zero air used as a carrier gas, Figure S2 (Johnson and Rella, 2017). To investigate how the
precision of the isotope values depends on the averaging time, Allan deviation (square root of Allan
variance) curves are shown in supplementary material Figure 3. All three isotope signatures of water
vapor show a similar pattern. The optimum precision is reached at averaging times of 16.7 minutes for
 $\delta^{18}O$ and δD and 15 minutes for $\delta^{17}O$ (supplementary material Figure S3). Note that the $\delta^{17}O$
335 measurements of water vapor are not calibrated to an international isotope scale for our experiments.

3.4. Leaf water extraction and isotope analysis

Leaf water was extracted by cryogenic vacuum distillation for 4 h at 60°C following a well-established
procedure (Wang and Yakir, 2000; Landais et al., 2006; West et al., 2006). The vial with the leaf was
frozen using a liquid nitrogen bath and connected to another empty vial by glass tubing. The system was
340 then evacuated using a membrane pump (KNF Neuberger, Germany), (Supplementary Figure S4). The
pressure was monitored with a Dual pressure sensor (DualTrans transducer, MKS, USA). After the target
vacuum was reached (1mbar or below) the extraction system was isolated from the pump. The vial
containing the leaf was placed into a heater block (ORI BLOCK DB-1, Techne, England) while the empty
vial was kept at liquid nitrogen temperature for 4 hr (Supplementary Figure S4). The extracted leaf water,
345 ~ 0.7 ml (determined based on weight by measuring the leaf weight before and after extraction), was
collected in a 2 ml vial (Autosampler vials, National Scientific, the Netherlands) using a pipette and kept
in the freezer at -20°C before isotopic analysis. The $\delta^{17}O$ and $\delta^{18}O$ of leaf water was determined at the
Laboratoire des Sciences du Climat et de l'Environnement laboratory using a fluorination technique as
described in (Barkan and Luz, 2005; Landais et al., 2006; 2008). Water was converted to H_2 and O_2 using
350 CoF_3 as fluorinating reagent and the O_2 was collected in a sample tube immersed in liquid Helium (-
270°C). Finally, $\delta^{17}O$ and $\delta^{18}O$ of O_2 were measured with an isotope ratio mass spectrometer



(ThermoQuest MAT 253 Finnigan, Germany) in dual inlet mode. The measurement reproducibility for two replicates is 0.015‰, 0.010‰ and 0.005‰ for $\delta^{17}\text{O}$, $\delta^{18}\text{O}$ and $\Delta^{17}\text{O}$, respectively.

355 **3.5. Carbon dioxide extraction and isotope analysis**

CO₂ was extracted from the air samples in a system made from electropolished stainless steel (Supplementary Figure S5). Our system used four commercial traps (MassTech, Bremen, Germany) which consist of a 1/8" inlet tube inserted within a 1/4" tube that is closed at the bottom. The first two traps were operated at dry ice temperature (-78°C) to remove moisture and some organics. The other two traps were operated at liquid nitrogen temperature (-196°C) to trap CO₂. The flow rate during extraction was 55 mL min⁻¹, controlled by a mass flow controller (Brooks Instruments, Holland). After processing usually about 2L of air, the remaining air was evacuated and the extracted CO₂ (together with N₂O and potentially other condensable gases) was cryogenically transferred into a break seal tube from which it could later be liberated for isotopic measurement. The reproducibility of the extraction system was 30 parts per million (ppm) for $\delta^{18}\text{O}$ and 7 ppm for $\delta^{13}\text{C}$ determined on 14 extractions (1 σ standard deviation for the 14 extractions, Supplementary Table S1).

The extracted CO₂ was first measured for $\delta^{13}\text{C}$ and $\delta^{18}\text{O}$ with a Delta^{Plus}XL isotope ratio mass spectrometer (IRMS) (Thermo Finnigan, Germany) in dual inlet mode. N₂O was not separated from CO₂ in our system and we apply constant corrections of 0.2‰ for $\delta^{13}\text{C}$ and 0.3‰ for $\delta^{18}\text{O}$ to correct for the N₂O interference as suggested by (Mook and Hoek, 1983). After the isotope measurement, the remaining gas in the bellow of the IRMS was frozen back into the break seal tube for the measurement of $\Delta^{17}\text{O}$. The $\Delta^{17}\text{O}$ of CO₂ was determined using the CO₂-O₂ exchange method (Mahata et al., 2013; Barkan et al., 2015; Adnew et al., 2019). A detailed description of the CO₂-O₂ exchange system at Utrecht University is given in (Adnew et al., 2019) and the method is only described here briefly. Equal amounts of CO₂ and O₂ were mixed in a quartz reactor containing a platinum sponge catalyst at the bottom and heated at 750°C for 2hrs. After isotope equilibration, the CO₂ was trapped at liquid nitrogen temperature, while the O₂ was collected with 1 pellet of 5Å molecular sieve (1.6 mm, Sigma Aldrich, USA) at liquid nitrogen temperature. The isotopic composition of the isotopically equilibrated O₂ was measured with a Delta^{Plus}XL isotope ratio mass spectrometer in dual inlet mode with reference to a pure O₂ calibration gas that has been assigned values of $\delta^{17}\text{O} = 9.254\text{‰}$ and $\delta^{18}\text{O} = 18.542\text{‰}$ by measurements of multiple aliquots by E. Barkan at the Hebrew University of Jerusalem. The reproducibility of the $\Delta^{17}\text{O}$ measurement was better than 10 ppm (Supplementary Table S1).

385 **3.6. Leaf cuvette model**

We used a simple leaf cuvette model to evaluate the dependence of $\Delta_A \Delta^{17}\text{O}$ on key parameters. In this model, the leaf is partitioned into three different compartments: the intercellular air space, the mesophyll cell, and the chloroplast, as shown in supplementary material Figure S6. For the calculations with this model, we assumed an infinite boundary layer conductance. The detailed description of the model and the python code is given in the supplementary material.



In the leaf cuvette model, we used a 100 ppm drawdown of CO₂, similar to the leaf exchange experiments, i.e., the CO₂ mole fraction decreases from 500 ppm in the entering air (c_e) to 400 ppm in the outgoing air (c_o), which is identical to the air surrounding the leaf (c_a) as a result of thorough mixing in the cuvette. The assimilation rate is set to 20.0 $\mu\text{mol m}^{-2}\text{s}^{-1}$. The leaf area and flowrate of air are set to 30 cm² and 0.7 L min⁻¹, respectively. The isotope composition of leaf water at the site where the H₂O-CO₂ exchange occurs is $\delta^{17}\text{O} = 5.39\text{‰}$ and $\delta^{18}\text{O} = 10.648\text{‰}$, which is the mean of the measured $\delta^{17}\text{O}$ and $\delta^{18}\text{O}$ values of bulk leaf water in our experiments. The leaf water temperature is set to 22°C (similar to the experiment). In the model, the $\delta^{18}\text{O}$ of the CO₂ entering the cuvette is set to 30.47‰ for all the simulations, as in the normal CO₂ experiments, but the assigned $\Delta^{17}\text{O}$ values ranges from -0.5‰ to 0.5‰ which encompasses both the stratospheric intrusion and combustion components. The corresponding $\delta^{17}\text{O}$ of the CO₂ entering the cuvette is calculated from the assigned $\delta^{18}\text{O}$ value (30.47‰) and $\Delta^{17}\text{O}$ values (-0.5‰ to 0.5‰). The schematic of the leaf cuvette model is shown in Figure S6 (supplementary material).

4. Results

4.1. Discrimination against ¹⁸O and ¹⁷O of CO₂

¹⁷O and ¹⁸O-photosynthetic discrimination ($\Delta_A^{17}\text{O}$ and $\Delta_A^{18}\text{O}$) for sunflower, ivy, and maize as a function of the c_m/c_a ratio is shown in Figure 4. $\Delta_A^{17}\text{O}$ and $\Delta_A^{18}\text{O}$ vary with c_m/c_a (the c_m is calculated using ¹⁸O isotope measurement of CO₂, see section 2.4) for all plant species investigated. For sunflower, we observe $\Delta_A^{18}\text{O}$ values between 29‰ and 64‰ for c_m/c_a between 0.54 and 0.86. Ivy shows a relatively little variation of $\Delta_A^{18}\text{O}$ around a mean of 22‰ for c_m/c_a between 0.48 and 0.58. For maize, $\Delta_A^{18}\text{O}$ is lower than for the C₃ plants measured in this study, with values between 10‰ and 20‰ for c_m/c_a between 0.15 and 0.37. As expected, for all species the behavior for $\Delta_A^{17}\text{O}$ is very similar to the one for $\Delta_A^{18}\text{O}$ (Figure 4b).

For sunflower changing the irradiance from 300 $\mu\text{mol m}^{-2}\text{s}^{-1}$ (low light, hereafter LL) to 1200 $\mu\text{mol m}^{-2}\text{s}^{-1}$ (high light, hereafter HL) causes average decreases of 12‰ for $\Delta_A^{17}\text{O}$ and 22‰ for $\Delta_A^{18}\text{O}$. For maize, the changes are only 2.2‰ for $\Delta_A^{17}\text{O}$ and 4.4‰ for $\Delta_A^{18}\text{O}$. For ivy, changing the light intensity does not significantly change the observed $\Delta_A^{17}\text{O}$ and $\Delta_A^{18}\text{O}$. The blue diamond points in Fig. 4 show results for $\Delta_A^{18}\text{O}$ and $\Delta_A^{17}\text{O}$ calculated using Farquhar model (Farquhar and Lloyd, 1993) (equation 7 for $\Delta_A^{18}\text{O}$). Overall, there is a good agreement between the calculated and the measured discrimination, but for the highest discriminations (high c_m/c_a ratios, LL experiments of sunflower) the calculations slightly underestimate the measured values. The Farquhar model fits well for both $\Delta_A^{17}\text{O}$ and $\Delta_A^{18}\text{O}$ with (R², root mean square error (RMSE)) values of (0.993, 0.6‰) for $\Delta_A^{17}\text{O}$ and (0.994, 1.2‰), for $\Delta_A^{18}\text{O}$, respectively. The solid lines in Figure 4 show results of leaf cuvette model calculations, where the dependence of $\Delta_A^{17}\text{O}$ and $\Delta_A^{18}\text{O}$ on c_m/c_a is explored for a set of calculations with otherwise fixed parameters. The model shows a good agreement with the experimental results except for ivy, where the model overestimates the discrimination.

4.2. Discrimination against ¹⁷O-excess of CO₂



The discrimination of photosynthesis against the ^{17}O -excess ($\Delta_A\Delta^{17}\text{O}$) of CO_2 is shown in Figure 5. $\Delta_A\Delta^{17}\text{O}$ was negative for all experiments and it depends strongly on the c_m/c_a ratio. For sunflower and
435 ivy, $\Delta_A\Delta^{17}\text{O}$ is also strongly dependent on the $\Delta^{17}\text{O}$ of CO_2 supplied to the cuvette, whereas no significant
dependence is found for maize. The leaf cuvette model results illustrate the shape of the dependence on
the c_m/c_a ratio and agree well with the experiments. For the leaf cuvette model, the $\Delta^{17}\text{O}$ value of the
water is assigned a constant value of -0.122‰ (average $\Delta^{17}\text{O}$ value for the bulk leaf water). Results from
the Farquhar model (equation 7 for $\Delta_A^{18}\text{O}_{\text{FM}}$ and analogous equation for $\Delta_A^{17}\text{O}_{\text{FM}}$) fit well with the
440 measurements ($R^2 = 0.959$, $\text{RMSE} = 0.1\text{‰}$) (Figure 5a, Figure S7 (supplementary material)). The RMSE
is lower than the measurement error for the $\Delta_A\Delta^{17}\text{O}$ in our experimental setup. Based on our measurement,
the error introduced in $\Delta_A\Delta^{17}\text{O}$ for the individual experiment is 0.25‰ (SD) calculated from the individual
errors of $\Delta_A^{17}\text{O}$ and $\Delta_A^{18}\text{O}$.

445 Figure 5b shows the same values of $\Delta_A\Delta^{17}\text{O}$ as a function of the difference between $\Delta^{17}\text{O}$ of CO_2 entering
the leaf and $\Delta^{17}\text{O}$ of leaf water at the evaporation site where $\text{CO}_2\text{-H}_2\text{O}$ exchange takes place ($\Delta^{17}\text{O}_a -$
 $\Delta^{17}\text{O}_{\text{wes}}$), for different c_m/c_a ratios. The leaf cuvette model results (solid lines in Figure 5b) suggest a linear
dependence between $\Delta_A\Delta^{17}\text{O}$ and $(\Delta^{17}\text{O}_a - \Delta^{17}\text{O}_{\text{wes}})$. The experimental results agree with the hypothesis
that $\Delta_A\Delta^{17}\text{O}$ is linearly dependent on $\Delta^{17}\text{O}_a - \Delta^{17}\text{O}_{\text{wes}}$ at a certain c_m/c_a ratio. Figure 6 shows the
450 corresponding relation where $\Delta_A\Delta^{17}\text{O}$ is divided by $\Delta^{17}\text{O}_a - \Delta^{17}\text{O}_m$. All the values follow the same
relationship with c_m/c_a ratio with an exponential function (equation 19). This function quantifies the
dependence of $\Delta_A\Delta^{17}\text{O}$ on c_m/c_a , and thus the effect of the diffusion of isotopically exchanged CO_2 back
to the atmosphere, which increased with increasing c_m/c_a ratio.

$$\frac{\Delta_A\Delta^{17}\text{O}}{\Delta^{17}\text{O}_a - \Delta^{17}\text{O}_m} = -0.150 \times \exp(3.707 \times c_m/c_a) + 0.028 \quad (19)$$

455

Figure 7 shows results from the leaf cuvette model that illustrates in more detail how $\Delta^{17}\text{O}_e$ and $\Delta^{17}\text{O}_{\text{wes}}$
affect $\Delta^{17}\text{O}_a$ and $\Delta_A\Delta^{17}\text{O}$ and their dependence on c_m/c_a . At lower c_m/c_a , only a very small fraction of CO_2
that has undergone isotopic equilibration in the mesophyll diffuses back to the atmosphere, and therefore
460 $\Delta^{17}\text{O}_a$ stays close to the incoming $\Delta^{17}\text{O}_e$, modified by the fractionation during CO_2 diffusion through the
stomata. Figure 7c confirms that indeed at low c_m/c_a , $\Delta_A\Delta^{17}\text{O}$ approaches the fractionation constant
expected for diffusion, -0.170‰ . This diffusional fractionation is independent of the isotopic composition
of the CO_2 entering the leaf, and therefore at low c_m/c_a , the $\Delta_A\Delta^{17}\text{O}$ curves for the different values of the
anomaly of the CO_2 entering the leaf converge. For a high c_m/c_a ratio, the back-diffusion of CO_2 that has
465 equilibrated with water becomes the dominant factor, and in this case, the isotopic composition of the
outgoing CO_2 converges towards this isotope value, independent of the isotopic composition of the
incoming CO_2 (Figure 7a). This can lead to a very wide range of values for the discrimination against
 $\Delta^{17}\text{O}$, because now the effect on $\Delta^{17}\text{O}$ of the ambient CO_2 depends strongly on the difference in isotopic
composition between incoming CO_2 and CO_2 in isotopic equilibrium with the leaf water.

470



In the model calculations shown in Fig. 7b and d, the isotopic composition of the water was changed in the model from $\Delta^{17}\text{O}_{\text{wes}} = -0.122\text{‰}$ to 0.300‰ , whereas all other parameters were kept the same. The value of $\Delta^{17}\text{O}_e$ for which $\Delta^{17}\text{O}_a$ does not depend on c_m/c_a is shifted accordingly, again being similar to $\Delta^{17}\text{O}_m$. At low c_m/c_a $\Delta_A\Delta^{17}\text{O}$ converges to the same value as in Fig 7 c), confirming the role of diffusion into the stomata as discussed above.

Figure 8 shows how $\delta^{18}\text{O}$ and $\Delta^{17}\text{O}$ varied in key compartments of the leaf cuvette system that determine the oxygen isotope effects associated with photosynthesis. The irrigation water has a $\Delta^{17}\text{O}$ value of 0.017 . The measured bulk leaf water is $6\text{--}16\text{‰}$ enriched in ^{18}O and its $\Delta^{17}\text{O}$ value is lower by -0.075 to -0.200‰ (mean value -0.121‰) than the irrigation water, calculated using a three-isotope slope of $\lambda_{\text{trans}} = 0.516$ at 80% humidity (Landais et al., 2006). $\Delta^{17}\text{O}$ of leaf water at the evaporation site, calculated from the transpired water, has slightly lower ^{17}O -excess, with values between -0.119‰ and -0.237 (average -0.184‰). Note that the bulk leaf water was not measured for all the experiments. For the experiments where the bulk leaf water is measured, $\Delta^{17}\text{O}$ of leaf water at the evaporation site ranges from -0.160‰ to -0.231 with an average value of $-0.190 \pm 0.020 \text{‰}$. The calculated isotopic composition of water at the exchange site was thus similar, but slightly lower in $\Delta^{17}\text{O}$ than the values measured for bulk leaf water. CO_2 exchanges with the water in the leaf with a well-established fractionation constant (equation 18) and a three-isotope slope of $\lambda_{\text{CO}_2\text{-H}_2\text{O}} = 0.5229$ (Barkan and Luz, 2012), leading to the lower $\Delta^{17}\text{O}$ values of the equilibrated CO_2 . In our experiments, the $\Delta^{17}\text{O}$ value of CO_2 in equilibrium with leaf water is lower than the $\Delta^{17}\text{O}$ value of CO_2 entering the leaf. The $\Delta^{17}\text{O}$ of the CO_2 in the intercellular air space between the two end members (the $\Delta^{17}\text{O}$ of the CO_2 entering the leaf and $\Delta^{17}\text{O}$ of the CO_2 in equilibrium with leaf water). This explains why the observed values of $\Delta_A\Delta^{17}\text{O}$ are negative for the experiments performed in this study.

5. Discussion

5.1. Discrimination against ^{17}O and ^{18}O of CO_2

The higher $\Delta_A^{18}\text{O}_{\text{obs}}$ and $\Delta_A^{17}\text{O}_{\text{obs}}$ values for sunflower compared to maize and ivy (Figure 4) is mainly due to a higher back-diffusion flux ($c_m/(c_a - c_m)$). The back-diffusion flux is higher for sunflower and ivy (C_3 plants) than for maize (C_4 plant), a consequence of the lower stomatal conductance (Gillon and Yakir, 2000b; Barbour et al., 2016) and higher assimilation rate of C_4 plants. In C_4 plants most of the CO_2 entering the stomata is carboxylated by PEPC resulting in a lower CO_2 mixing ratio in the mesophyll which results in a lower back-diffusion flux. The increase of assimilation rate with higher light intensity also explains the decreases of $\Delta_A^{18}\text{O}_{\text{obs}}$ and $\Delta_A^{17}\text{O}_{\text{obs}}$ with decreasing c_m/c_a ratio for maize and sunflower, which is observed most clearly for sunflower. A similar trend of increase in $\Delta_A^{18}\text{O}_{\text{obs}}$ with an increase in c_m/c_a ratio has been reported in previous studies (Gillon and Yakir, 2000a, b; Osborn et al., 2017). For ivy, $\Delta_A^{18}\text{O}_{\text{obs}}$ and $\Delta_A^{17}\text{O}_{\text{obs}}$ do not decrease with an increase in irradiance. The change in assimilation rate with irradiance is small, thus CO_2 mole fraction in the mesophyll cell will not decrease strongly and the effect on the back diffusion is smaller than the variability in $\Delta_A^{18}\text{O}_{\text{obs}}$ and $\Delta_A^{17}\text{O}_{\text{obs}}$ of different leaves of the same plant.



515 The leaf cuvette model results shown in Figure 4 agree well with the measurements for sunflower and maize, but overestimate $\Delta_A^{18}\text{O}_{\text{obs}}$ and $\Delta_A^{17}\text{O}_{\text{obs}}$ for ivy. This is due to relatively higher $\delta^{17}\text{O}$ and $\delta^{18}\text{O}$ values of leaf water used in the leaf cuvette model calculations than the $\delta^{17}\text{O}$ and $\delta^{18}\text{O}$ values at the evaporation site. The Farquhar model (Equation 7) uses the individual values for each experiment, and agrees well with the experimental results for ivy, confirming that this is the cause of the discrepancy in the cuvette model.

520 In our experiments, photosynthesis causes enrichment in $\delta^{17}\text{O}$ and $\delta^{18}\text{O}$ of atmospheric CO_2 for both C_3 and C_4 plants, i.e. positive values of $\Delta_A^{17}\text{O}$ and $\Delta_A^{18}\text{O}$. In principle, $\Delta_A^{17}\text{O}$ and $\Delta_A^{18}\text{O}$ can also be negative if the $\delta^{17}\text{O}_m$ and $\delta^{18}\text{O}_m$ are depleted relative to the ambient CO_2 . This is in contrast to $\Delta_A^{13}\text{C}$, which will always be positive since it is determined by the fractionation due to the PEPC and RuBisCO enzyme activity (Figure S8 and S9, supplementary material). In general, in our experiments, the values for $\Delta_A^{17}\text{O}$ and $\Delta_A^{18}\text{O}$ are about five times larger than the relative difference between the $\delta^{17}\text{O}$ and $\delta^{18}\text{O}$ of the CO_2 entering and leaving the cuvette, respectively (Figure S10 and S11, supplementary material). This is easy to understand from the definition of Δ_A . Taking $\Delta_A^{18}\text{O}$ as an example, $\Delta_A^{18}\text{O}_{\text{obs}} = \frac{\zeta(\delta^{18}\text{O}_a - \delta^{18}\text{O}_e)}{1 + \delta^{18}\text{O}_a - \zeta(\delta^{18}\text{O}_a - \delta^{18}\text{O}_e)} \approx \zeta(\delta^{18}\text{O}_a - \delta^{18}\text{O}_e)$ and in our experiments, $\zeta = c_e / (c_e - c_a) \approx 500 / (500 - 400) = 5$.

5.2. Discrimination against the ^{17}O -excess of CO_2

530 Unlike ivy and sunflower, maize does not show a significant change in $\Delta_A \Delta^{17}\text{O}$ when CO_2 gases with different $\Delta^{17}\text{O}$ are supplied to the plant. The C_4 plant maize has a small back-diffusion flux due to its high assimilation rate and low stomatal conductance, leading to a low c_m/c_a ratio. At these low c_m/c_a ratios, $\Delta_A^{18}\text{O}$ and $\Delta_A^{17}\text{O}$ (equation 7 for $\Delta_A^{18}\text{O}$) are close to the weighted fractionation due to diffusion through boundary layer and stomata, $\Delta_A^{18}\text{O} = a_{18\text{bs}}$ and $\Delta_A^{17}\text{O} = a_{17\text{bs}}$ (Appendix 3 equation A3.3 and A3.9, respectively). As a result, $\Delta_A \Delta^{17}\text{O}$ of CO_2 is dominated by the fractionation due to diffusion (Figure 7 c and d, inset). In general, the effect of diffusion on $\Delta^{17}\text{O}$ of atmospheric CO_2 can be expressed as follows:

$$\Delta^{17}\text{O}_{\text{Modified}} = \Delta^{17}\text{O}_a + (\lambda_{\text{ref}} - \lambda_{\text{diffusion}}) \times \ln \alpha_{\text{diffusion}} \quad (20)$$

540 where $\Delta^{17}\text{O}_a$ is the $\Delta^{17}\text{O}$ of the CO_2 surrounding the leaf, $\Delta^{17}\text{O}_{\text{modified}}$ is the $\Delta^{17}\text{O}$ of the CO_2 modified due to diffusional fractionation and $\lambda_{\text{diffusion}}$, λ_{ref} and $\alpha_{\text{diffusion}}$ are the oxygen three-isotope relationships during diffusion from the $\text{CO}_2\text{-H}_2\text{O}$ exchange site to the atmosphere, the reference slope used and the fractionation against ^{18}O for CO_2 during diffusion through the stomata. Using the values $\lambda_{\text{RL}} = 0.528$, $\lambda_{\text{diffusion}} = 0.509$ (Young et al., 2002) and $\alpha_{\text{diffusion}} = 0.9912$ (Farquhar and Lloyd, 1993), the effect of diffusional fractionation on the $\Delta^{17}\text{O}$ of atmospheric CO_2 is -168 ppm regardless of the anomaly of the CO_2 entering the leaf, and the model results confirm this at low c_m/c_a ratio (Figure 7 c and d, inset).

545 At a high c_m/c_a ratio, $\Delta^{17}\text{O}_a$ is dominated by the back diffusion of CO_2 that has equilibrated with water to the cuvette. As a consequence, $\Delta^{17}\text{O}_a$ converges to a common value that is independent of the anomaly of



the CO₂ entering the cuvette and is determined by the isotopic composition of leaf water. The end member appears to be equal to the $\Delta^{17}\text{O}$ of CO₂ in equilibrium with leaf water, $\Delta^{17}\text{O}_m$ (Fig. 7). When $\Delta^{17}\text{O}_a = \Delta^{17}\text{O}_m$, $\Delta^{17}\text{O}_a$ does not change with c_m/c_a , indicating that in this case the $\Delta^{17}\text{O}$ of the CO₂ diffusing back from the leaf is the same as the $\Delta^{17}\text{O}$ CO₂ entering the leaf.

\bar{a}_{18} is the overall discrimination occurring during the diffusion of ¹²C¹⁸O¹⁶O from the ambient air to the CO₂-H₂O exchange site. In our study \bar{a}_{18} ranges from 5‰ to 7.2‰, lower than the literature estimate of 7.4‰ (Farquhar et al., 1993). \bar{a}_{18} depends on the ratio of stomatal conductance, which is associated with a strong fractionation of 8.8‰ to mesophyll conductance with an associated fractionation of only 0.8‰. Therefore, the higher the ratio (g_s/g_{m18}) the lower the \bar{a}_{18} (Table S2, supplementary material). The difference in \bar{a}_{18} of 2.4‰ between the literature value of 7.4‰ and the lowest \bar{a}_{18} estimate in this study will introduce an error of only 46 ppm in the $\Delta^{17}\text{O}$ value (see equation 19). The uncertainty \bar{a}_{18} has lower influence on the $\Delta_A\Delta^{17}\text{O}$ of C₃ plants compared to C₄ plants since the diffusional fractionation is less important at the higher c_m/c_a ratio where C₃ plants operate.

5.3. Global average value of $\Delta_A\Delta^{17}\text{O}$ and $\Delta^{17}\text{O}$ isoflux

We can use the established relationship between $\Delta_A\Delta^{17}\text{O}$ and $\Delta^{17}\text{O}_a - \Delta^{17}\text{O}_{\text{wes}}$ for a certain c_m/c_a ratio to provide a leaf-scale based bottom-up estimate for the global effect of photosynthesis on $\Delta^{17}\text{O}$ in atmospheric CO₂. For this, we use results from a recent modeling study, which provides global average values for CO₂ and leaf water ($\Delta^{17}\text{O}(\text{CO}_2) = -0.168\text{‰}$, $\Delta^{17}\text{O}(\text{H}_2\text{O}_{\text{-leaf}}) = -0.067\text{‰}$; (Koren et al., 2019); Figure S12 and 13, supplementary material). The $\Delta^{17}\text{O}(\text{CO}_2)$ values agree well with the limited amount of available measurements (Table 1).

To extrapolate $\Delta_A\Delta^{17}\text{O}$ determined in the leaf scale experiments to the global scale, c_m/c_a ratios of 0.7 and 0.3 are used for C₃ and C₄ plants, respectively, similar to previous studies (Hoag et al., 2005). From SIBCASA model results we obtained an annual variability of c_m/c_a values with a standard deviation of 0.12 and 0.17 for C₄ and C₃ plants respectively (Figure S14, supplementary material) (Schaefer et al., 2008; Koren et al., 2019). We assigned this variability worst case estimates for the error in c_m/c_a as shown in the light orange and light pink shaded areas in figure 5b. Based on the linear dependency of $\Delta_A\Delta^{17}\text{O}$ and $\Delta^{17}\text{O}_a - \Delta^{17}\text{O}_{\text{wes}}$, we estimated the $\Delta_A\Delta^{17}\text{O}$ for tropospheric CO₂ based on the $\Delta^{17}\text{O}$ of leaf water and c_m/c_a ratio. In Figure 5b, the dashed black vertical line indicates $\Delta^{17}\text{O}_a - \Delta^{17}\text{O}_{\text{wes}}$ obtained from the 3D global model (Koren et al., 2019). The results of the global estimate and parameters used for the extrapolation of leaf scale study to the global scale are summarized in Table 1.

The $\delta^{17}\text{O}$ value of atmospheric CO₂ (21.53‰) is calculated from the global $\delta^{18}\text{O}$ and $\Delta^{17}\text{O}$ values (41.5‰ and -0.168‰, respectively) (Koren et al., 2019). The $\delta^{17}\text{O}$ and $\delta^{18}\text{O}$ values of global mean leaf water are calculated from the soil water. A global mean $\delta^{18}\text{O}$ value of soil water is -8.4‰ assuming soil water is similar to precipitation (Bowen and Revenaugh, 2003; Koren et al., 2019). The $\delta^{17}\text{O}$ value of soil water is -4.4‰, calculated using equation 20 (Luz and Barkan, 2010).



$$\ln(\delta^{17}\text{O}_{soil} + 1) = 0.528 \times \ln(\delta^{18}\text{O}_{soil} + 1) + 0.033 \quad (21)$$

$\delta^{17}\text{O}$ and $\delta^{18}\text{O}$ of leaf water are calculated from $\delta^{17}\text{O}$ and $\delta^{18}\text{O}$ of soil water with fractionation factors of 1.0043 and 1.0084 and, respectively (Hofmann et al., 2017; Koren et al., 2019). The fractionation factor for $\delta^{17}\text{O}$ is calculated using $\alpha^{17} = (\alpha^{18})^{\lambda_{trans}}$ with a three-isotope exponent for transpiration of $\lambda_{trans} = 0.516$, assuming relative humidity to be 80% (Landais et al., 2006). The $\delta^{17}\text{O}$ and $\delta^{18}\text{O}$ values of global mean leaf water are then -0.136‰ and -0.131‰ , respectively. Thus, the difference between global atmospheric CO_2 and leaf water is $\delta^{17}\text{O}_{\text{CO}_2 - \text{water}} = 21.666\text{‰}$ and $\delta^{18}\text{O}_{\text{CO}_2 - \text{water}} = 41.631\text{‰}$. This yields $\Delta^{17}\text{O}_{\text{CO}_2 - \text{water}} = -0.101\text{‰}$, and this value is indicated as dashed black line in figure 4. The grey shaded area indicates the propagated error using the standard deviation of the relevant parameters in 180×360 grid boxes for 12 months of leaf water and 45×60 grid boxes for 24 months for CO_2 (Koren et al., 2019). In Fig. 5b, the intersection between the dashed black vertical line and the discrimination lines for the representative c_m/c_a ratios of C_3 and C_4 plants correspond to the $\Delta_A \Delta^{17}\text{O}$ value of C_3 and C_4 plants. For C_4 plants ($c_m/c_a = 0.3$) this yields $\Delta_A \Delta^{17}\text{O} = -0.3\text{‰}$ (gray dashed line in Figure 5b) and for C_3 plants ($c_m/c_a = 0.7$), $\Delta_A \Delta^{17}\text{O} = -0.65\text{‰}$ (black dashed line in Figure 5b).

Three main factors contribute to the uncertainty of the extrapolated $\Delta_A \Delta^{17}\text{O}$ value. The first is due to measurement error which contributes 0.25‰ (standard error for individual experiments). The second factor is the uncertainty in the difference between $\Delta^{17}\text{O}$ of atmospheric CO_2 and leaf water. Statistics for all 45×60 grid boxes for 24 months (2012-2013) show a range of -0.218‰ to -0.151‰ for $\Delta^{17}\text{O}$ of atmospheric CO_2 with a mean of -0.168‰ and a standard deviation of 0.013‰ (Figure S12, supplementary material). Statistics for all 180×360 grid boxes for 12 months show a range of -0.236‰ and -0.027‰ for $\Delta^{17}\text{O}$ of the leaf water (Figure S13, supplementary material). The mean is -0.067‰ with a standard deviation of 0.041‰ . The third uncertainty in the extrapolation of $\Delta^{17}\text{O}$ comes from the uncertainty in the c_m/c_a ratio. For C_3 and C_4 plants, these errors are indicated by the light orange and light blue shadings in Figure 5b.

Taking these uncertainties into account leads to a mean value of $\Delta_A \Delta^{17}\text{O} = -0.3 \pm 0.18\text{‰}$ for C_4 plants and $\Delta_A \Delta^{17}\text{O} = -0.65 \pm 0.18\text{‰}$ for C_3 plants. Using assimilation weighted fractions of 23% for C_4 and 77% for C_3 vegetation (Still et al., 2003), the global mean value of $\Delta_A \Delta^{17}\text{O}$ obtained from equation 14 is $-0.57 \pm 0.14\text{‰}$. The $\Delta_A \Delta^{17}\text{O}$ isoflux due to photosynthesis is calculated using a GPP value of 120 PgCyr^{-1} (Beer et al., 2010) and $A = 0.88 \times \text{GPP}$, resulting in an isoflux of $-60 \pm 15\text{‰ PgCyr}^{-1}$ globally. This is the first global estimate of $\Delta_A \Delta^{17}\text{O}$ based on direct measurements of the discrimination during assimilation. Our value is in good agreement with the previous model estimates. (Hofmann et al., 2017) estimated an isoflux ranging from -42 to -92‰ PgCyr^{-1} (converted to a reference line with $\lambda = 0.528$) using an average c_m/c_a ratio of 0.7 for both C_4 and C_3 plants and $\Delta^{17}\text{O}$ of -0.147‰ for atmospheric CO_2 . A previous model-estimated value (Hoag et al., 2005) is -47‰ PgCyr^{-1} (with $\lambda = 0.528$), derived with a more simple model and using $\Delta^{17}\text{O}$ of -0.146‰ with c_m/c_a ratio of 0.33 and 0.66 for C_4 and C_3 plants, respectively.

The main uncertainty in the extrapolation of $\Delta_A \Delta^{17}\text{O}$ from the leaf experiments to the global scale is the uncertainty in the c_m/c_a ratio. The error from the uncertainty in c_m/c_a ratio increases when the relative



625 difference in $\Delta^{17}\text{O}$ between CO_2 and leaf water increases (Figure 5b). It is difficult to determine a single
representative c_m value for different plants because this value would need to be properly weighted with
temperature, irradiance, CO_2 mole fraction and other environmental factors (Flexas et al.,
2008;2012;Shrestha et al., 2019). Recent developments in laser spectroscopy techniques (McManus et
al., 2005;Nelson et al., 2008;Tuzson et al., 2008;Kammer et al., 2011) might enable more and easier
630 measurements of c_m/c_a both in the laboratory and under field conditions. This could lead to a better
understanding of variations in the c_m/c_a ratio among plant species and, temporally, spatially and
environmentally.

6. Conclusions

635 In order to investigate the effect of photosynthetic gas exchange on the $\Delta^{17}\text{O}$ of atmospheric CO_2 at the
leaf level, gas exchange experiments were carried out with isotopically normal and slightly anomalous
(^{17}O -enriched) CO_2 in leaf cuvettes using two C_3 plants (sunflower and ivy) and one C_4 plant (maize).
Results for ^{13}C , ^{17}O and ^{18}O agree with results reported in the literature previously. For $\Delta^{17}\text{O}$, our
experiments confirm that two parameters determine the effect of photosynthesis on CO_2 : 1) the $\Delta^{17}\text{O}$
640 difference between the incoming CO_2 and CO_2 in equilibrium with leaf water and 2) the c_m/c_a ratio, which
determines the degree of back-flux of isotopically exchanged CO_2 from the mesophyll to the atmosphere.
In addition, at low c_m/c_a ratios, $\Delta_A\Delta^{17}\text{O}$ is mainly influenced by the diffusional fractionation. Under our
experimental conditions, the isotopic effect increased with c_m/c_a , e.g. $\Delta_A\Delta^{17}\text{O}$ was -0.3‰ and -0.65‰ for
maize and sunflower with c_m/c_a ratios of 0.3 and 0.7, respectively. However, experiments with mass
645 independently fractionated CO_2 demonstrate that the results depend strongly on the $\Delta^{17}\text{O}$ difference
between the incoming CO_2 and CO_2 in equilibrium with leaf water. This is supported by calculations with
a leaf cuvette model. Our results confirm that the formalism developed by Farquhar and others is also
applicable to the evaluation of $\Delta^{17}\text{O}$.

650 Results from the leaf exchange experiments were upscaled to the global atmosphere using modeled values
for $\Delta^{17}\text{O}$ of leaf water and CO_2 , which results in $\Delta_A\Delta^{17}\text{O} = -0.57 \pm 0.14\text{‰}$ and a value for the $\Delta^{17}\text{O}$ isoflux
of $-60 \pm 15\text{‰ PgCyr}^{-1}$. This is the first study that provides such an estimated based on direct leaf chamber
measurements, and the results agree with previous $\Delta^{17}\text{O}$ calculations. The largest contribution to the
uncertainty originates from uncertainty in the c_m/c_a ratio and the largest contributions to the isoflux come
655 from C_3 plants, which have both a higher share of the total assimilation and higher discrimination. $\Delta_A\Delta^{17}\text{O}$
is less sensitive to c_m/c_a ratios at lower values of c_m/c_a , for instance for C_4 plants, maize.

$\Delta^{17}\text{O}$ of tropospheric CO_2 is controlled by photosynthetic gas exchange, respiration, soil invasion, and
stratospheric influx. The stratospheric flux is well established and the effect of photosynthetic gas
660 exchange can now be quantified more precisely. To untangle the contribution of each component to the
 $\Delta^{17}\text{O}$ atmospheric CO_2 we recommend measuring the effects of foliage respiration and soil invasion both
in the laboratory and at the ecosystem scale.

665 Code and data availability.



The data used in this study are included in the paper either with figures or tables. The python code for the cuvette model is provided as supplementary material.

Author contributions.

670 GAA and TR designed the main idea of the study. GAA and TP designed the leaf cuvette setup. TP monitors plant growth. GAA and TR designed the CO₂ extraction and CO₂-H₂O exchange system. GAA conducted all the measurements. GK provided the leaf cuvette model. WP enabled the work within the ASICA project. All authors discussed the results at different steps of the project. GAA and TR prepared the manuscript with contributions from all the co-authors.

Competing interests.

675 The authors declare that they have no conflict of interest

Acknowledgments

680 The authors thank Leonard I. Wassenaar and Stefan Terzer-Wassmuth from the International Atomic and Energy Agency, Vienna for supplying water standards. The authors thank Eugeni Barkan and Rolf Vieten from the Hebrew University of Jerusalem for calibration of our O₂ and CO₂ working gases. We are grateful to Amaelle Landais from Laboratoire des Sciences Du Climat et de l'Environnement Université Paris-Saclay for measuring the $\Delta^{17}\text{O}$ of leaf water samples for our study. The authors thank Amzad Laskar for useful discussion during the design of the experiment. This work is funded by the EU ERC
685 project ASICA.

References

- 690 Adnew, G. A., Hofmann, M. E. G., Paul, D., Laskar, A., Surma, J., Albrecht, N., Pack, A., Schwieters, J., Koren, G., Peters, W., and Röckmann, T.: Determination of the triple oxygen and carbon isotopic composition of CO₂ from atomic ion fragments formed in the ion source of the 253 Ultra High-Resolution Isotope Ratio Mass Spectrometer, *Rapid Commun. Mass. Sp.*, 33, 17, 2019.
- Badger, M. R., and Price, G. D.: The role of carbonic anhydrase in photosynthesis, *Annu. Rev. Plant Biol.*, 45, 23, 1994.
- 695 Barbour, M. M., Evans, J. R., Simonin, K. A., and Caemmerer, S. V.: Online CO₂ and H₂O oxygen isotope fractionation allows estimation of mesophyll conductance in C₄ plants, and reveals that mesophyll conductance decreases as leaves age in both C₄ and C₃ plants, *New Phytol.*, 14, 2016.
- Barkan, E., and Luz, B.: High precision measurements of ¹⁷O/¹⁶O and ¹⁸O/¹⁶O ratios in H₂O, *Rapid Commun. Mass. Sp.*, 19, 3737-3742, 10.1002/rcm.2250, 2005.
- 700 Barkan, E., and Luz, B.: Diffusivity fractionations of H₂¹⁶O/H₂¹⁷O and H₂¹⁶O/H₂¹⁸O in air and their implications for isotope hydrology, *Rapid Commun. Mass. Sp.*, 21, 6, 2007.
- Barkan, E., and Luz, B.: The relationships among the three stable isotopes of oxygen in air, seawater and marine photosynthesis, *Rapid Commun. Mass. Sp.*, 25, 2, 2011.
- Barkan, E., and Luz, B.: High-precision measurements of ¹⁷O/¹⁶O and ¹⁸O/¹⁶O ratios in CO₂, *Rapid Commun. Mass. Sp.*, 26, 2733-2738, 10.1002/rcm.6400, 2012.



- 705 Barkan, E., Musan, I., and Luz, B.: High-precision measurements of $\delta^{17}\text{O}$ and ^{17}O -excess of NBS19 and NBS18, *Rapid Commun. Mass. Sp.*, 29, 2219-2224, 10.1002/rcm.7378, 2015.
- Beer, C., Reichstein, M., Tomelleri, E., Ciais, P., Jung, M., Carvalhais, N., Rodenbeck, C., Arain, M. A., Baldocchi, D., Bonan, G. B., Bondeau, A., Cescatti, A., Lasslop, G., Lindroth, A., Lomas, M., Luyssaert, S., Margolis, H., Oleson, K. W., Rouspard, O., Veenendaal, E., Viovy, N., Williams, C., Woodward, F. I., and Papale, D.: Terrestrial gross carbon dioxide uptake: global distribution and covariation with climate, *Science*, 329, 834-838, 10.1126/science.1184984, 2010.
- 710 Boering, K. A.: Observations of the anomalous oxygen isotopic composition of carbon dioxide in the lower stratosphere and the flux of the anomaly to the troposphere, *Geophysical Research Letters*, 31, 10.1029/2003gl018451, 2004.
- Booth, B. B. B., Jones, C. D., Collins, M., Totterdell, I. J., Cox, P. M., Sitch, S., Huntingford, C., Betts, R. A., Harris, G. R., and Lloyd, J.: High sensitivity of future global warming to land carbon cycle processes, *Environmental Research Letters*, 7, 10.1088/1748-9326/7/2/024002, 2012.
- 715 Bottinga, Y., and Craig, H.: Oxygen isotope fractionation between CO_2 and water, and the isotopic composition of marine atmospheric CO_2 , *Earth Planet Sc. Lett.*, 5, 10, 1968.
- Bowen, G. J., and Revenaugh, J.: Interpolating the isotopic composition of modern meteoric precipitation, *Water Resour. Res.*, 39, 2003.
- 720 Brand, W. A., Assonov, S. S., and Coplen, T. B.: Correction for the ^{17}O interference in $\delta^{13}\text{C}$ measurements when analyzing CO_2 with stable isotope mass spectrometry (IUPAC Technical Report), *Pure Appl. Chem.*, 82, 1719-1733, 10.1351/pac-rep-09-01-05, 2010.
- Breninkmeijer, C. A. M., Kraft, P., and Mook, W. G.: Oxygen isotope fractionation between CO_2 and H_2O , *Chem. Geol.*, 41, 8, 1983.
- 725 Caemmerer, S. V., and Farquhar, G. D.: Some relationships between the biochemistry of photosynthesis and the gas exchange of leaves, *Planta*, 153, 11, 1981.
- Caemmerer, S. V., Ghannoum, O., Pengelly, J. J. L., and Cousins, A. B.: Carbon isotope discrimination as a tool to explore C_4 photosynthesis, *J. Exp. Bot.*, 65, 3459, 2014.
- Cao, X., and Liu, Y.: Equilibrium mass-dependent fractionation relationships for triple oxygen isotopes, *Geochimica et Cosmochimica Acta*, 75, 7435-7445, 10.1016/j.gca.2011.09.048, 2011.
- 730 Cernusak, L. A., Barbour, M. M., Arndt, S. K., Cheesman, A. K., English, N. B., Feild, T. S., Helliker, B. R., Holloway-Phillips, M. M., Holtum, J. A., Kahmen, A., McInerney, F. A., Munksgaard, N. C., Simonin, K. A., Song, X., Stuart-Williams, H., West, J. B., and Farquhar, G. D.: Stable isotopes in leaf water of terrestrial plants, *Plant Cell Environ.*, 39, 1087-1102, 10.1111/pce.12703, 2016.
- 735 Ciais, P., Denning, A. S., Tans, P. P., Berry, J. A., Randall, D. A., Collatz, G. J., Sellers, P. J., White, J. W. C., Trolrier, M., Meijer, H. A. J., Francey, R. J., Monfray, P., and Heimann, M.: A three-dimensional synthesis study of $\delta^{18}\text{O}$ in atmospheric CO_2 : 1. Surface fluxes, *J. Geophys. Res-Atmos.*, 102, 5857-5872, 10.1029/96jd02360, 1997a.
- Ciais, P., Tans, P. P., Denning, A. S., Francey, R. J., Trolrier, M., Meijer, H. A. J., White, J. W. C., Berry, J. A., Randall, D. A., and Collatz, G. J.: A three-dimensional synthesis study of $\delta^{18}\text{O}$ in atmospheric CO_2 : 2. Simulations with the TM2 transport model, *J. Geophys. Res-Atmos.*, 102, 10, 1997b.
- 740 Cousins, A. B., Mullendore, D. L., and Sonawane, B. V.: Recent developments in mesophyll conductance in C_3 , C_4 and CAM plants *Plant J.*, 2020.
- Craig, H., and Gordon, L. I.: Deuterium and oxygen 18 variations in the ocean and the marine atmosphere, *Consiglio nazionale delle ricerche, Laboratorio de geologia nucleare Pisa*, 1965.
- 745 Cuntz, M., Ciais, P., Hoffmann, G., Allison, C. E., Francey, R. J., Knorr, W., Tans, P. P., White, J. W. C., and Levin, I.: A comprehensive global three-dimensional model of $\delta^{18}\text{O}$ in atmospheric CO_2 : 2. Mapping the atmospheric signal *J. Geophys. Res-Atmos.*, 108, 2003a.
- Cuntz, M., Ciais, P., Hoffmann, G., and Knorr, W.: A comprehensive global three-dimensional model of $\delta^{18}\text{O}$ in atmospheric CO_2 : 1. Validation of surface processes, *J. Geophys. Res-Atmos.*, 108, 24, 2003b.
- 750 Cuntz, M.: A dent in carbon's gold standard, *Nature*, 477, 547-548, 2011.
- DiMario, R. J., Quebedeaux, J. C., Longstreth, D. J., Dassanayake, M., Hartman, M. M., and Moroney, J. V.: The cytoplasmic carbonic anhydrases βCA_2 and βCA_4 are required for optimal plant growth at low CO_2 , *Plant Physiol.*, 171, 13, 2016.
- Ehleringer, J. R., and Monson, R. K.: Evolutionary and ecological aspects of photosynthetic pathway variation, *Annu. Rev. Ecol. Syst.*, 24, 28, 1993.



- 755 Ehleringer, J. R., and Cerling, T. E.: C₃ and C₄ photosynthesis, *Encyclopedia of Global Environmental Change*, 2, 4, 2002.
Evans, J. R., Sharkey, T. D., Berry, J. A., and Farquhar, G. D.: Carbon isotope discrimination measured concurrently with gas exchange to investigate CO₂ diffusion in leaves of higher plants, *Funct. Plant Biol.*, 13, 11, 1986.
Evans, J. R., Kaldenhoff, R., Genty, B., and Terashima, I.: Resistances along the CO₂ diffusion pathway inside leaves *J. Exp. Bot.*, 60, 13, 2009.
- 760 Fabre, N., Reiter, I. M., Becuwe-Linka, N., Genty, B., and Rumeau, D.: Characterization and expression analysis of genes encoding alpha and beta carbonic anhydrases in *Arabidopsis*, *Plant Cell Environ.*, 30, 617-629, 10.1111/j.1365-3040.2007.01651.x, 2007.
Farquhar, D. G., O'Leary, M. H., and J. A. Berry: On the relationship between carbon isotope discrimination and intercellular carbon dioxide concentration in leaves *Australian Journal of Plant Physiology*, 9, 16, 1982.
- 765 Farquhar, D. G., and Lloyd, J.: Carbon and oxygen isotope effects in the exchange of carbon dioxide between terrestrial plants and the atmosphere, *Stable isotopes and plant carbon-water relations*, Academic Press Inc., London, 47 pp., 1993.
Farquhar, G. D., and Richards, R. A.: Isotopic composition of plant carbon correlates with water-use efficiency of wheat genotypes, *Functional Plant Biology*, 11, 11, 1984.
Farquhar, G. D., Ehleringer, J. R., and Hubick, K. T.: Carbon isotope discrimination and photosynthesis, *Annu. Rev. Plant Physiol. Plant Mol. Biol.*, 40, 34, 1989a.
- 770 Farquhar, G. D., Hubick, K. T., Condon, A. G., and Richards, R. A.: Carbon isotope fractionation and plant water-use efficiency. In *Stable isotopes in ecological research*, edited by: Billings, W. D., Golley, F., Lange, O. L., Olson, J. S., and Remmert, H., Springer, New York, NY, 19 pp., 1989b.
Farquhar, G. D., Lloyd, J., Taylor, J. A., Flanagan, L. B., Syvertsen, J. P., Hubick, K. T., Wong, S. C., and Ehleringer, J. R.: Vegetation effects on the isotope composition of oxygen in atmospheric CO₂, *Nature*, 363, 4, 1993.
- 775 Farquhar, G. D., and Gan, K. S.: On the progressive enrichment of the oxygen isotopic composition of water along a leaf, *Plant, Cell & Environment*, 26, 18, 2003.
Farquhar, G. D., and Cernusak, L. A.: Ternary effects on the gas exchange of isotopologues of carbon dioxide, *Plant Cell Environ.*, 35, 1221-1231, 10.1111/j.1365-3040.2012.02484.x, 2012.
- 780 Flanagan, L. B., Comstock, J. P., and Ehleringer, J. R.: Comparison of modeled and observed environmental influences on the stable oxygen and hydrogen isotope composition of leaf water in *Phaseolus vulgaris* L., *Plant Physiology*, 96, 8, 1991.
Flanagan, L. B.: Environmental and biological influences on the stable oxygen and hydrogen isotopic composition of leaf water, in: *Stable isotopes and plant carbon-water relations*, Elsevier, 1993.
Flanagan, L. B., and Ehleringer, J. R.: Ecosystem-atmosphere CO₂ exchange: interpreting signals of change using stable isotope ratios, *Trends Ecol. Evol.*, 13, 4, 1998.
- 785 Flexas, J., Ribas-Carbo, M., Diaz-Espejo, A., Galmes, J., and Medrano, H.: Mesophyll conductance to CO₂: current knowledge and future prospects, *Plant Cell Environ.*, 31, 19, 2008.
Flexas, J., Barbour, M. M., Brendel, O., Cabrera, H. M., Carriqui, M., Díaz-Espejo, A., Douthe, C., Dreyer, E., Ferrio, J. P., and Gago, J.: Mesophyll diffusion conductance to CO₂: an unappreciated central player in photosynthesis *Plant Sci.*, 193, 14, 2012.
- 790 Francey, R. J., and Tans, P. P.: Latitudinal variation in oxygen-18 of atmospheric CO₂, *Nature*, 327, 2, 1987.
Fredeen, A. L., Gamon, J. A., and Field, C. B.: Responses of photosynthesis and carbohydrate-partitioning to limitations in nitrogen and water availability in field-grown sunflower *Plant Cell Environ.*, 14, 7, 1991.
Friedli, H., Siegenthaler, U., Rauber, D., and Oeschger, H.: Measurements of concentration, ¹³C/¹²C and ¹⁸O/¹⁶O ratios of tropospheric carbon dioxide over Switzerland, *Tellus B*, 8, 1987.
- 795 Gan, K. S., Wong, S. C., Yong, J. W. H., and Farquhar, G. D.: ¹⁸O spatial patterns of vein xylem water, leaf water, and dry matter in cotton leaves, *Plant Physiol.*, 130, 13, 2002.
Gan, K. S., Wong, S. C., Yong, J. W. H., and Farquhar, G. D.: Evaluation of models of leaf water ¹⁸O enrichment using measurements of spatial patterns of vein xylem water, leaf water and dry matter in maize leaves, *Plant Cell Environ.*, 26, 16, 2003.
- 800 Gillon, J., and Yakir, D.: Influence of carbonic anhydrase activity in terrestrial vegetation on the ¹⁸O content of atmospheric CO₂, *Science*, 291, 3, 2001.
Gillon, J. S., and Yakir, D.: Naturally low carbonic anhydrase activity in C₄ and C₃ plants limits discrimination against C¹⁸O during photosynthesis, *Plant Cell Environ.*, 23, 12, 2000a.



- 805 Gillon, J. S., and Yakir, D.: Internal conductance to CO₂ diffusion and C¹⁸O discrimination in C₃ leaves, *Plant Physiol.*, 123, 11, 2000b.
- Harwood, K. G., Gillon, J. S., Griffiths, H., and Broadmeadow, M. S. J.: Diurnal variation of Δ¹³CO₂, ΔC¹⁸O¹⁶O and evaporative site enrichment of δH₂¹⁸O in *Piper aduncum* under field conditions in *Trinidad Plant Cell Environ.*, 21, 14, 1998.
- 810 Hoag, K. J., Still, C. J., Fung, I. Y., and Boering, K. A.: Triple oxygen isotope composition of tropospheric carbon dioxide as a tracer of terrestrial gross carbon fluxes, *Geophys. Res. Lett.*, 32, 10.1029/2004gl021011, 2005.
- Hofmann, M. E. G., Horváth, B., Schneider, L., Peters, W., Schützenmeister, K., and Pack, A.: Atmospheric measurements of Δ¹⁷O in CO₂ in Göttingen, Germany reveal a seasonal cycle driven by biospheric uptake, *Geochim. Cosmochim. Ac.*, 199, 143-163, 10.1016/j.gca.2016.11.019, 2017.
- 815 Jähne, B., Münnich, K. O., Bössinger, R., Dutzi, A., Huber, W., and Libner, P.: Jähne, Bernd, et al. "On the parameters influencing air-water gas exchange, *Journal of Geophysical Research, Oceans*, 92(C2), 12, 10.1029/JC092iC02p01937, 1987.
- Johnson, J. E., and Rella, C. W.: Effects of variation in background mixing ratios of N₂, O₂, and Ar on the measurement of δ¹⁸O-H₂O and δ²H-H₂O values by cavity ring-down spectroscopy, *Atmos. Meas. Tech.*, 10, 18, 2017.
- Jung, M., Schwalm, C., Migliavacca, M., Walther, S., Camps-Valls, G., Koirala, S., Anthoni, P., Besnard, S., Bodesheim, P., and Carvalhais, N.: Scaling carbon fluxes from eddy covariance sites to globe: synthesis and evaluation of the FLUXCOM approach. In open review for *Biogeosciences.*, *Biogeosciences*, 2019.
- 820 Kammer, A., Tuzson, B., Emmenegger, L., Knohl, A., Mohn, J., and Hagedorn, F.: Application of a quantum cascade laser-based spectrometer in a closed chamber system for real-time δ¹³C and δ¹⁸O measurements of soil-respired CO₂, *Agr. Forest. Meteorol.*, 151, 9, 2011.
- Kawagucci, S., Tsunogai, U., Kudo, S., Nakagawa, F., Honda, H., Aoki, S., Nakazawa, T., Tsutsumi, M., and Gamo, T.: Long-term observation of mass-independent oxygen isotope anomaly in stratospheric CO₂, *Atmos. Chem. Phys.*, 8, 8, 2008.
- 825 Koren, G., Schneider, L., Velde, I. R. v. d., Schaik, E. v., Gromov, S. S., Adnew, G. A., D.J.Mrozek, Hofmann, M. E. D., Liang, M.-C., Mahata, S., Bergamaschi, P., Laan-Luijkx, I. T. v. d., Krol, M. C., Röckmann, T., and Peters, W.: Global 3-D Simulations of the Triple Oxygen Isotope Signature Δ¹⁷O in Atmospheric CO₂ *J. Geophys. Res-Atmos.*, 124, 28, 2019.
- 830 Lämmerzahl, P., Röckmann, T., and Brenninkmeijer, C. A. M.: Oxygen isotope composition of stratospheric carbon dioxide, *Geophys. Res. Lett.*, 29, 10.1029/2001gl014343, 2002.
- Landais, A., Barkan, E., Yakir, D., and Luz, B.: The triple isotopic composition of oxygen in leaf water, *Geochim. Cosmochim. Ac.*, 70, 4105-4115, 10.1016/j.gca.2006.06.1545, 2006.
- 835 Landais, A., Barkan, E., and Luz, B.: Record of δ¹⁸O and ¹⁷O-excess in ice from Vostok Antarctica during the last 150,000 years, *Geophys. Res. Lett.*, 35, 10.1029/2007gl032096, 2008.
- Laskar, A. H., Mahata, S., and Liang, M.-C.: Identification of anthropogenic CO₂ using triple oxygen and clumped isotopes, *Environ. Sci. Technol.*, 50, 18, 10.1021/acs.est.6b02989, 2016.
- Liang, M.-C., Blake, G. A., Lewis, B. R., and Yung, Y. L.: Oxygen isotopic composition of carbon dioxide in the middle atmosphere, *PNAS*, 104, 4, 2006.
- 840 Liang, M.-C., and Mahata, S.: Oxygen anomaly in near surface carbon dioxide reveals deep stratospheric intrusion, *Sci. Rep.*, 5, 11352, 10.1038/srep11352, 2015.
- Liang, M.-C., Mahata, S., Laskar, A. H., and Bhattacharya, S. K.: Spatiotemporal variability of oxygen isotope anomaly in near surface air CO₂ over urban, semi-urban and ocean areas in and around Taiwan, *Aerosol Air Qual. Res.*, 17, 24, 2017a.
- 845 Liang, M.-C., Mahata, S., Laskar, A. H., Thiemens, M. H., and Newman, S.: Oxygen isotope anomaly in tropospheric CO₂ and implications for CO₂ residence time in the atmosphere and gross primary productivity, *Sci. Rep.*, 7, 13180, 2017b.
- Luz, B., and Barkan, E.: Variations of ¹⁷O/¹⁶O and ¹⁸O/¹⁶O in meteoric waters *Geochim. Cosmochim. Ac.*, 74, 10, 2010.
- Lyons, J. R.: Transfer of mass-independent fractionation in ozone to other oxygen-containing radicals in the atmosphere, *Geophys. Res. Lett.*, 28, 3231-3234, 10.1029/2000gl012791, 2001.
- 850 Mahata, S., Bhattacharya, S. K., Wang, C. H., and Liang, M.-C.: Oxygen isotope exchange between O₂ and CO₂ over hot platinum: an innovative technique for measuring Δ¹⁷O in CO₂, *Anal. Chem.*, 85, 6894-6901, 10.1021/ac4011777, 2013.
- Mason, E. A., and Marrero, T. R.: The diffusion of atoms and molecules, *Advances in Atomic and Molecular Physics*, 6, 77, 10.1016/S0065-2199(08)60205-5, 1970.
- Matsuhisa, Y., Goldsmith, J. R., and Clayton, R. N.: Mechanisms of hydrothermal crystallization of quartz at 250 °C and 15 kbar, *Geochimica et Cosmochimica Acta*, 42, 9, 1978.



- 855 McKinney, R. C., McCrea, M. J., Epstein, S., Allen, H. A., and Urey, H. C.: Improvements in mass spectrometers for the measurement of small differences in isotope abundance ratios *Review of Scientific Instruments*, 21, 6, 10.1063/1.1745698, 1950.
- McManus, J. B., Nelson, D. D., Shorter, J. H., Jimenez, R., Herndon, S., Saleska, S., and Zahniser, M.: A high precision pulsed quantum cascade laser spectrometer for measurements of stable isotopes of carbon dioxide, *J. Mod. Optic.*, 52, 12, 2005.
- 860 Meijer, H., and Li, W.: The use of electrolysis for accurate ^{17}O and ^{18}O isotope measurements in water isotopes, *Isotopes Environ. Health Stud.*, 34, 20, 1998.
- Merlivat, L.: Molecular diffusivities of H_2^{16}O , HD^{16}O , and H_2^{18}O in gases, *J. Chem. Phys.*, 69, 7, 1978.
- Millenaar, F. F., Marjolein, C. C. H., Berkel, Y. E. M. J. v., Welschen, R. A. M., Pierik, R., Voeselek, L. A. J. C., and Peeters, A. J. M.: Ethylene-induced differential growth of petioles in *Arabidopsis*. Analyzing natural variation, response kinetics, and regulation *Plant Physiol.*, 137, 10, 2005.
- 865 Miller, J. B., Yakir, D., White, J. W. C., and Tans, P. P.: Measurement of $^{18}\text{O}/^{16}\text{O}$ in the soil-atmosphere CO_2 flux, *Global Biogeochem. Cy.*, 13, 13, 1999.
- Mook, W. G., and Hoek, S. V. d.: The N_2O correction in the carbon and oxygen isotopic analysis of atmospheric CO_2 , *Chem. Geol.*, 41, 5, 1983.
- 870 Nelson, D. D., McManus, J. B., Herndon, S., Zahniser, M. S., Tuzson, B., and Emmenegger, L.: New method for isotopic ratio measurements of atmospheric carbon dioxide using a $4.3\ \mu\text{m}$ pulsed quantum cascade laser *Appl. Phys. B-Lasers. O.*, 90, 8, 2008.
- O'Leary, M. H.: Measurement of the isotope fractionation associated with diffusion of carbon dioxide in aqueous solution, *The Journal of Physical Chemistry*, 88, 2, 1984.
- 875 Osborn, H. L., Alonso-Cantabrana, H., Sharwood, R. E., Covshoff, S., Evans, J. R., Furbank, R. T., and Caemmerer, S. v.: Effects of reduced carbonic anhydrase activity on CO_2 assimilation rates in *Setaria viridis*: a transgenic analysis, *J. Exp. Bot.*, 68, 11, 2017.
- Pack, A., and Herwartz, D.: The triple oxygen isotope composition of the Earth mantle and understanding $\Delta^{17}\text{O}$ variations in terrestrial rocks and minerals *Earth. Planet. Sc. Lett.*, 390, 7, 2014.
- 880 Peylin, P., Ciais, P., Denning, A. S., Tans, P. P., Berry, J. A., and White, J. W.: A 3-dimensional study of $\delta^{18}\text{O}$ in atmospheric CO_2 : contribution of different land ecosystems, *Tellus B*, 51, 25, 1999.
- Pons, T. L., and Welschen, R. A. M.: Overestimation of respiration rates in commercially available clamp-on leaf chambers. Complications with measurement of net photosynthesis, *Plant, Cell and Environment*, 25, 5, 2002.
- Pons, T. L., Flexas, J., Caemmerer, S., Evans, J. R., Genty, B., Ribas-Carbo, M., and Brugnoli, E.: Estimating mesophyll conductance to CO_2 : methodology, potential errors, and recommendations *J. Exp. Bot.*
- 885 , 60, 7, 2009.
- Sage, R. F., and Monson, R. K.: *C₄ plant biology*, Elsevier, 1998.
- Schaefer, K., Collatz, G. J., Tans, P., Denning, A. S., Baker, I., Berry, J., Prihodko, L., Suits, N., and Philpott, A.: Combined simple biosphere/Carnegie-Ames-Stanford approach terrestrial carbon cycle model, *J. Geophys. Res-Bioge.*
- 890 , 113, 2008.
- Sharp, Z. D., Wostbrock, J. A. G., and Pack, A.: Mass-dependent triple oxygen isotope variations in terrestrial materials, *Geochemical Perspectives Letters*, 27-31, 10.7185/geochemlet.1815, 2018.
- Shrestha, A., Song, X., and Barbour, M. M.: The temperature response of mesophyll conductance, and its component conductances, varies between species and genotypes, *Photosynth. Res.*, 18, 2019.
- 895 Sitch, S., Friedlingstein, P., Gruber, N., Jones, S. D., Murray-Tortarolo, G., Ahlström, A., Doney, S. C., Graven, H., Heinze, C., and Huntingford, C.: Recent trends and drivers of regional sources and sinks of carbon dioxide, *Biogeosciences*, 12, 26, 2015.
- Still, C. J., Berry, J. A., Collatz, G. J., and DeFries, R. S.: Global distribution of C_3 and C_4 vegetation: Carbon cycle implications, *Global Biogeochem. Cy.*, 17, 6-1-6-14, 10.1029/2001gb001807, 2003.
- 900 Thiemens, M. H., Jackson, T., Mauersberger, K., Schüler, B., and Morton, J.: Oxygen isotope fractionation in stratospheric CO_2 , *Geophys. Res. Lett.*, 18, 669-672, 1991.
- Thiemens, M. H., Jackson, T., Zipf, E. C., Erdman, P. W., and Egmond, C. v.: Carbon dioxide and oxygen isotope anomalies in the mesosphere and stratosphere, *Science* 270, 3, 1995.
- Thiemens, M. H.: Mass-independent isotope effects in planetary atmospheres and the early solar system, *Science*, 283, 4, 1999.



- 905 Thiemens, M. H.: History and Applications of Mass-Independent Isotope Effects, *Annu. Rev. Earth Planet. Sci.*, 34, 62, 10.1146/, 2006.
- Thiemens, M. H., Chakraborty, S., and Jackson, T. L.: Decadal $\Delta^{17}\text{O}$ record of tropospheric CO_2 : Verification of a stratospheric component in the troposphere, *J. Geophys. Res. Atmos.*, 119, 8, 10.1002/2013JD020317, 2013.
- 910 Thiemens, M. K., Chakraborty, S., and Jackson, T. L.: Decadal $\Delta^{17}\text{O}$ record of tropospheric CO_2 : Verification of a stratospheric component in the troposphere, *J. Geophys. Res.-Atmos.*, 119, 8, 2014.
- Tuzson, B., Mohn, J., Zeeman, M. J., Werner, R. A., Eugster, W., Zahniser, M. S., Nelson, D. D., McManus, J. B., and Emmenegger, L.: High precision and continuous field measurements of $\delta^{13}\text{C}$ and $\delta^{18}\text{O}$ in carbon dioxide with a cryogen-free QCLAS, *Appl. Phys. B-Lasers O.*, 92, 7, 2008.
- 915 Ubierna, N., Holloway-Phillips, M.-M., and Farquhar, G. D.: Using stable carbon isotopes to study C_3 and C_4 photosynthesis: models and calculations *Photosynthesis*, 41 pp., 2018.
- Ubierna, N., Cernusak, L. A., Holloway-Phillips, M., Busch, F. A., Cousins, A. B., and Farquhar, G. D.: Critical review: incorporating the arrangement of mitochondria and chloroplasts into models of photosynthesis and carbon isotope discrimination, *Photosynth. Res.*, 141, 26, 2019.
- 920 Vogel, J. C., Grootes, P. M., and Mook, W. G.: Isotopic fractionation between gaseous and dissolved carbon dioxide, *Z. Physik*, 230, 13, 1970.
- Wang, X.-F., and Yakir, D.: Using stable isotopes of water in evapotranspiration studies, *Hydrol. Process.*, 14, 14, 2000.
- Wassenaar, L. I., Terzer-Wassmuth, S., Douence, C., Araguas-Araguas, L., Aggarwal, P. K., and Coplen, T. B.: Seeking excellence: An evaluation of 235 international laboratories conducting water isotope analyses by isotope-ratio and laser-absorption spectrometry, *Rapid Commun Mass Spectrom*, 32, 393-406, 10.1002/rcm.8052, 2018.
- 925 Weijde, T. v. d., Kamei, K. C. L. A., Torres, A. F., Vermerris, W., Dolstra, O., Visser, R. G. F., and Trindade, L. M.: The potential of C_4 grasses for cellulosic biofuel production, *Front. Plant. Sci.*, 4, 107, 2013.
- Welp, L. R., Keeling, R. F., Meijer, H. A. J., Bollenbacher, A. F., Piper, S. C., Yoshimura, K., Francey, R. J., Allison, C. A., and Wahlen, M.: Interannual variability in the oxygen isotopes of atmospheric CO_2 driven by El Niño, *Nature*, 477, 579-582, 10.1038/nature10421, 2011.
- 930 West, A. G., Patrickson, S. J., and Ehleringer, J. R.: Water extraction times for plant and soil materials used in stable isotope analysis, *Rapid Commun Mass Spectrom*, 20, 1317-1321, 10.1002/rcm.2456, 2006.
- Wingate, L., Ogée, J., Cuntz, M., Genty, B., Reiter, I., Seibt, U., Yakir, D., Maseyk, K., Pendall, E. G., Barbour, M. M., Mortazavi, B., Burlett, R., Peylin, P., Miller, J., Mencuccini, M., Shim, J. H., Hunt, J., and Grace, J.: The impact of soil microorganisms on the global budget of $\delta^{18}\text{O}$ in atmospheric CO_2 , *Proceedings of the National Academy of Sciences*, 106, 4, 2009.
- 935 Yakir, D.: Oxygen-18 of leaf water: a crossroad for plant-associated isotopic signals, *Stable isotopes: integration of biological, ecological and geochemical processes*, 21, 1998.
- Yakir, D., and Sternberg, L. S. L.: The use of stable isotopes to study ecosystem gas exchange, *Oecologia*, 123, 4, 2000.
- 940 Young, E. D., Galy, A., and Nagahara, H.: Kinetic and equilibrium mass-dependent isotope fractionation laws in nature and their geochemical and cosmochemical significance, *Geochim. Cosmochim. Ac.*, 66, 9, 2002.

Appendix A1

945 Leaf exchange parameters are calculated following (Caemmerer and Farquhar, 1981). The transpiration rate (E) is calculated from the air flowrate, leaf area and concentration of water vapor entering and leaving the cuvette as:

$$E = \frac{u_e}{s} \times \left(\frac{w_a - w_e}{1 - w_a} \right) \quad (\text{A1.1})$$

where w_a , w_e , are the mole fractions of water leaving (a) or entering (e) the cuvette, u_e is flowrate of air entering the cuvette and s is the leaf surface area. The assimilation rate (A) is calculated as:



$$A = \frac{u_e}{s} \times \left(c_e - c_a \times \left(\frac{1 - w_e}{1 - w_a} \right) \right) \quad (\text{A1.2})$$

950 where c_e and c_a are the mole fractions of CO_2 leaving and entering the cuvette. The total conductance for water vapor (g_{wa}^t) is calculated as:

$$g_{wa}^t = E \times \left(\frac{1 - \left(\frac{w_i + w_a}{2} \right)}{w_i - w_a} \right) \quad (\text{A1.3})$$

where w_i and w_a are the water vapor mole fraction in the intercellular air space (calculated assuming saturation at ambient temperature) and the mole fraction of water vapor leaving the cuvette. The mole fraction of CO_2 in the intercellular air space is calculated as:

955

$$c_i = \frac{\left(g_{ac}^t - \frac{E}{2} \right) \times c_a - A}{\left(g_{ac}^t - \frac{E}{2} \right)} \quad (\text{A1.4})$$

where g_{ca}^t is the total conductance for CO_2 . For a detailed derivation of the leaf exchange parameters, the reader is referred to (Caemmerer and Farquhar, 1981).

Appendix A2

Isotopic composition of water at the evaporation site

960

Using mass balance between the air entering and leaving the cuvette, the $\delta^{18}\text{O}$ of the transpired ($\delta^{18}\text{O}_{\text{trans}}$) water is calculated according to (Harwood et al., 1998):

$$\delta^{18}\text{O}_{\text{trans}} = \left(\frac{w_a}{w_a - w_e} \right) \times (\delta^{18}\text{O}_{w_a} - \delta^{18}\text{O}_{w_e}) + \delta^{18}\text{O}_{w_e} \quad (\text{A2.1})$$

965 where $\delta^{18}\text{O}_{w_e}$ and $\delta^{18}\text{O}_{w_a}$ are $\delta^{18}\text{O}$ values of water vapor entering and leaving the cuvette and w_a and w_e are the mole fractions of water vapor entering and leaving the cuvette. $\delta^{17}\text{O}$ is calculated based on the triple isotope relationship for transpiration, $\alpha^{17} = (\alpha^{18})^{\lambda_{\text{trans}}}$ where $\lambda_{\text{trans}} = 0.522 - 0.008 \times h$ (Landais et al., 2006). h is relative humidity, $0.3 \leq h \leq 1$, which is calculated as $h = \frac{w_a}{w_i}$, w_i is the saturation mole fraction of water vapor in the intercellular air space.

970

Leaf water at the site of evaporation is enriched during evaporation and/or transpiration since the heavier isotopologues diffuse slower than the lighter ones (Flanagan et al., 1991; Farquhar et al., 1993; Flanagan, 1993; Yakir and Sternberg, 2000). The degree isotopic enrichment due to the phase change from water to vapor (evaporation) and diffusion is described by the modified Craig and Gordon model (Craig and Gordon, 1965) including resistance to boundary layer and stomata diffusion as described by (Farquhar

975



980

et al., 1989b; Flanagan et al., 1991; Flanagan, 1993). Measurement of the isotopic composition of air entering and leaving the cuvette allows determining the isotopic composition of water at the evaporation site even if it is not in steady state as described in (Farquhar et al., 1989b; Flanagan et al., 1991; Harwood et al., 1998). The $\delta^{18}\text{O}$ of leaf water at the site of evaporation ($\delta^{18}\text{O}_{\text{wes}}$) is:

$$\delta^{18}\text{O}_{\text{wes}} = \delta^{18}\text{O}_{\text{trans}} + \varepsilon^{18}_{\text{k}} + \varepsilon^{18}_{\text{equ}} + \frac{W_{\text{a}}}{W_{\text{i}}} \times (\delta^{18}\text{O}_{\text{wa}} - \varepsilon^{18}_{\text{k}} + \delta^{18}\text{O}_{\text{trans}}) \quad (\text{A2.2})$$

where $\varepsilon^{18}_{\text{k}}$ and $\varepsilon^{18}_{\text{equ}}$ are the kinetic fractionation of water vapor in air and the equilibrium fractionation between liquid and gas phase water, respectively. The equilibrium fractionation is temperature dependent (Bottinga and Craig, 1968) and calculated as:

$$\varepsilon^{18}_{\text{equ}} = 2.644 - 3.206 \times \left(\frac{10^3}{T}\right) + 1.534 \times \left(\frac{10^6}{T}\right) \quad (\text{A2.3})$$

985

where T is the temperature in Kelvin. H_2^{18}O has lower vapor pressure and diffuses slower than H_2^{16}O (Farquhar and Lloyd, 1993). The kinetic isotope effect due to diffusion ε_{k} , is the weighted sum of the fractionations of water isotopologues during diffusion through the stomata in the air (ε_{ks}) and through the boundary layer (ε_{kb}) (Farquhar and Lloyd, 1993). According to (Merlivat, 1978; Barkan and Luz, 2007), the fractionation factor for H_2^{18}O as it diffuses through stomata is 28‰ ($\varepsilon^{18}_{\text{ks}}$). According to (Farquhar

990

and Lloyd, 1993) $\varepsilon_{\text{kb}} = (\varepsilon_{\text{ks}})^{\frac{2}{3}}$, i.e., the fractionation factor as H_2^{18}O diffuses through the boundary layer is 19‰ ($\varepsilon^{18}_{\text{kb}}$). The fractionation factors for H_2^{17}O for diffusion through stomata and boundary layer are 14.6‰ and 9.7‰, respectively (Barkan and Luz, 2007). The kinetic fractionation of water vapor as it diffuses through stomata and boundary layer is given by equation A2.4 (Farquhar and Lloyd, 1993)

$$\varepsilon^{18}_{\text{k}} = \frac{28 \times g_{\text{b}} + 19 \times g_{\text{s}}}{g_{\text{b}} + g_{\text{s}}} \quad (\text{A2.4})$$

995

where g_{b} and g_{s} are boundary layer conductance and stomatal conductance respectively. $\delta^{17}\text{O}_{\text{wes}}$ can be calculated using a similar equation as $\delta^{18}\text{O}_{\text{wes}}$ if $\delta^{17}\text{O}_{\text{wa}}$ and $\delta^{17}\text{O}_{\text{we}}$ are known, for this study we calculated $\delta^{17}\text{O}_{\text{wes}}$ assuming the irrigation water is the same with soil water.

$$\delta^{17}\text{O}_{\text{wes}} = \left(\frac{\delta^{18}\text{O}_{\text{wes}} + 1}{\delta^{18}\text{O}_{\text{IRW}} + 1}\right)^{\lambda_{\text{trans}}} \times (\delta^{17}\text{O}_{\text{IRW}} + 1) - 1 \quad (\text{A2.5})$$

000 Appendix 3

Mole fraction of CO_2 at the $\text{CO}_2\text{-H}_2\text{O}$ exchange site

$\delta^{18}\text{O}_{\text{i}}$ is $\delta^{18}\text{O}$ of CO_2 in the intercellular airspace, calculated as (Farquhar and Cernusak, 2012):

005



$$\delta^{18}\text{O}_i = \frac{\delta^{18}\text{O}_{i0} + t^{18} \times \left(\delta^{18}\text{O}_A \times \left(\frac{c_a}{c_i} + 1 \right) - \delta^{18}\text{O}_a \times \frac{c_a}{c_i} \right)}{1 + t^{18}} \quad (\text{A3.1})$$

where the ternary correction factor t^{18} is calculated as:

$$t^{18} = \frac{(1 + a_{18bs}) \times E}{2g_{ac}} \quad (\text{A3.2})$$

010 g_{ac} is the conductance as CO_2 diffuses through the boundary layer and stomata, a_{18bs} is the weighted ^{18}O fractionation for CO_2 diffusion across the boundary layer and stomata in series.

$$a_{18bs} = \frac{(c_a - c_s) \times a_{18b} + (c_s - c_i) \times a_{18s}}{c_a - c_i} \quad (\text{A3.3})$$

The $\delta^{18}\text{O}_{i0}$ is the $\delta^{18}\text{O}$ of CO_2 in the intercellular air spaces ignoring ternary correction and it is given by (Farquhar and Cernusak, 2012).

$$\delta^{18}\text{O}_{i0} = \delta^{18}\text{O}_A \times \left(1 - \frac{c_a}{c_i} \right) \times (1 + a_{18bs}) + \frac{c_a}{c_i} \times (\delta^{18}\text{O}_a - a_{18bs}) + a_{18bs} \quad (\text{A3.4})$$

015 where a_{18w} is the ^{18}O fractionation of CO_2 for dissolution and diffusion in water (0.8‰) and a_{18s} and a_{18b} are the ^{18}O fractionation of CO_2 as it diffuses through stomata (8.8‰) and the boundary layer (5.8‰), respectively (Farquhar et al., 1982; Farquhar and Lloyd, 1993). The oxygen isotope composition of the assimilated CO_2 is calculated from a mass balance using the mole fraction and isotope composition of CO_2 entering and leaving the cuvette as:

$$\delta^{18}\text{O}_A = \frac{\delta^{18}\text{O}_a - \Delta_A^{18}\text{O}}{\Delta_A^{18}\text{O} + 1} \quad (\text{A3.5})$$

Similar to the derivation shown in the main paper for $\delta^{18}\text{O}$, the mole fraction of CO_2 at the $\text{CO}_2\text{-H}_2\text{O}$ exchange site can be calculated from $\delta^{17}\text{O}$ as:

$$c_m = c_i \left(\frac{\delta^{17}\text{O}_i - a_{17w} - \delta^{17}\text{O}_A \times (1 + a_{17w})}{\delta^{17}\text{O}_m - a_{17w} - \delta^{17}\text{O}_A \times (1 + a_{17w})} \right) \quad (\text{A3.6})$$

025 where $\delta^{17}\text{O}_{i\text{CO}_2}$ is $\delta^{17}\text{O}$ of CO_2 in the intercellular airspace including ternary correction (t^{17}), calculated as:

$$\delta^{17}\text{O}_i = \frac{\delta^{17}\text{O}_{i0} + t^{17} \times \left(\delta^{17}\text{O}_A \times \left(\frac{c_a}{c_i} + 1 \right) - \delta^{17}\text{O}_o \times \frac{c_a}{c_i} \right)}{1 + t^{17}} \quad (\text{A3.7})$$



$$t^{17} = \frac{(1 + a_{17bs}) \times E}{2g_{ac}} \quad (\text{A3.8})$$

030 Here a_{17bs} is the weighted discrimination of $C^{16}O^{17}O$ diffusion across the boundary layer and stomata in series respectively and is given by:

$$a_{17bs} = \frac{(c_a - c_s) \times a_{17b} + (c_s - c_i) \times a_{17s}}{c_a - c_i} \quad (\text{A3.9})$$

$\delta^{17}O_{io}$ is the $\delta^{17}O$ value of the CO_2 in the intercellular air spaces ignoring ternary correction and it is calculated as:

$$\delta^{17}O_{io} = \delta^{17}O_A \times \left(1 - \frac{c_a}{c_i}\right) \times (1 + \bar{a}_{17}) + \frac{c_a}{c_i} \times (\delta^{17}O_a - \bar{a}_{17}) + \bar{a}_{17} \quad (\text{A3.10})$$

035

where \bar{a}_{17} is the ^{17}O fractionation of CO_2 during diffusion across boundary layer, stomata, cell wall and plasma membrane in series, similar to $\delta^{18}O$.

$$\bar{a}_{17} = \frac{(c_a - c_s) \times a_{17b} + (c_s - c_i) \times a_{17s} + (c_i - c_m) \times a_{17w}}{c_a - c_m} \quad (\text{A3.11})$$

040 The ^{18}O fractionation ($\alpha^{18}-1$) for dissolution is -0.8% (Vogel.J.C. et al., 1970). The corresponding ^{17}O fractionation is -0.418% , calculated from the ^{18}O fractionation due to equilibrium dissolution using $\lambda_{CO_2-H_2O}$ is 0.5229 (Barkan and Luz, 2012). Assuming the ^{17}O fractionation during diffusion in water is the same as the fractionation in the $^{13}CO_2$ (Farquhar and Lloyd, 1993) and using the average fractionation determined for $^{13}CO_2$ is 0.8% (0.7% (O'Leary, 1984) and 0.9% (Jähne et al., 1987)). The ^{17}O fractionation due to the sum of the equilibrium dissolution and diffusion in water is then $a_{17w} = 0.382\%$. Similar to
 045 (Farquhar and Lloyd, 1993), using the principle of binary diffusivities (Mason and Marrero, 1970), a_{17s} and a_{17b} are 4.4% and 2.9% using the power of $2/3$ relationship between the boundary layer and stomatal conductance fractionation ($\alpha_b = \alpha_s^{2/3}$) obtained by (Farquhar and Lloyd, 1993).

050 For calculating the isotopic composition at the site of oxygen isotope exchange, we assume that the isotopic composition of CO_2 is fully equilibrated with water at the evaporation site. This includes the implicit assumption that the isotopic composition of the leaf water at the CO_2-H_2O exchange site is the same as at the site of evaporation. The $\delta^{17}O$ of CO_2 at the CO_2-H_2O exchange site ($\delta^{17}O_m$) is then calculated using the triple oxygen isotope ratio relationship, $\alpha^{17} = (\alpha^{18})^{\lambda_{CO_2-H_2O}}$.

$$\delta^{17}O_m = \left(\frac{\delta^{18}O_m + 1}{\delta^{18}O_{wes} + 1}\right)^{\lambda_{CO_2-H_2O}} \times (\delta^{17}O_{wes} + 1) - 1 \quad (\text{A3.12})$$

055

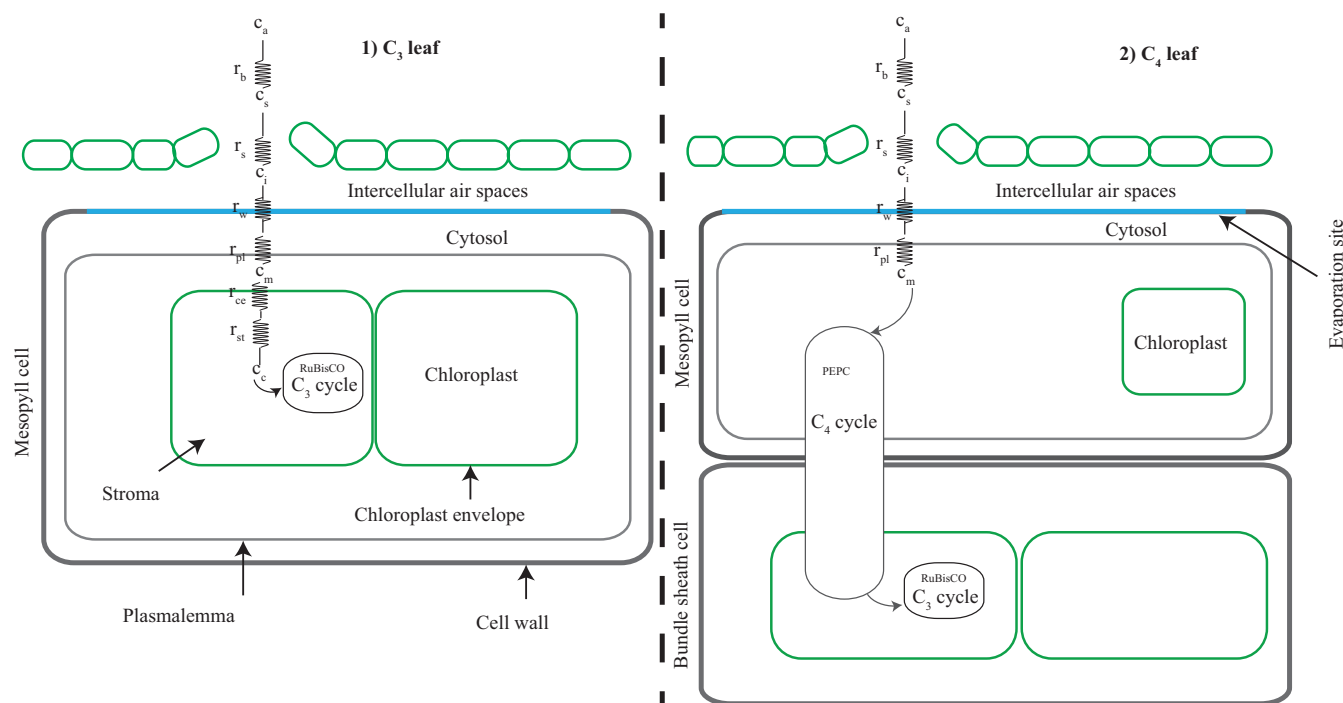


where $\lambda_{CO_2-H_2O}$ is 0.5229 (Barkan and Luz, 2012). Similar to $\delta^{18}O$, the $\delta^{17}O$ value of the assimilated CO_2 is calculated from a mass balance using the mole fraction and isotope composition of CO_2 entering and leaving the cuvette as:

$$\delta^{17}O_A = \frac{\delta^{17}O_a - \Delta_A^{17}O}{\Delta_A^{17}O + 1} \quad (A3.13)$$

060

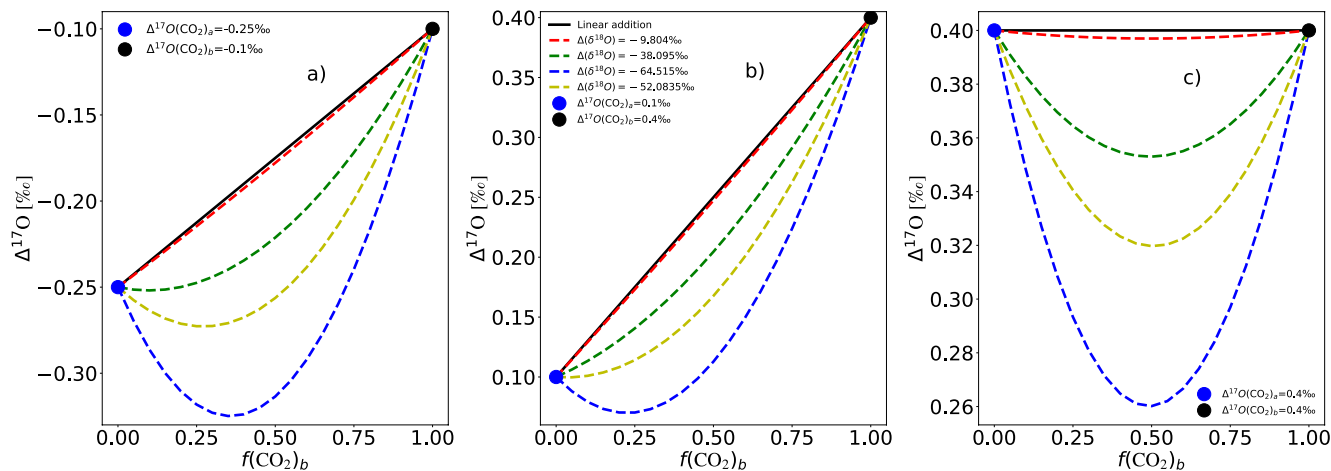
065



070

075

Figure 1 A simplistic 2-D schematic of CO_2 fluxes in a C_3 and C_4 leaf modified from (Cousins et al., 2020). During photosynthesis, ambient CO_2 (c_a) diffuses into the leaf intercellular spaces (c_i) through the boundary layer (r_b) and stomata (r_s). c_s is the mole fraction of CO_2 in the leaf surrounding. In a C_3 leaf (1) the resistances for CO_2 diffusion from the intercellular air space to RuBisCO in the chloroplast (c_c) is the wall (r_{wall}), the plasmalemma (r_{pl}), the chloroplast envelope (r_{ce}) and the stroma (r_{st}) resistance. In a C_4 leaf (2) the resistances for CO_2 diffusion to PEPC in the cytosol (c_m) is the wall (r_{wall}) and the plasmalemma (r_{pl}) resistances.

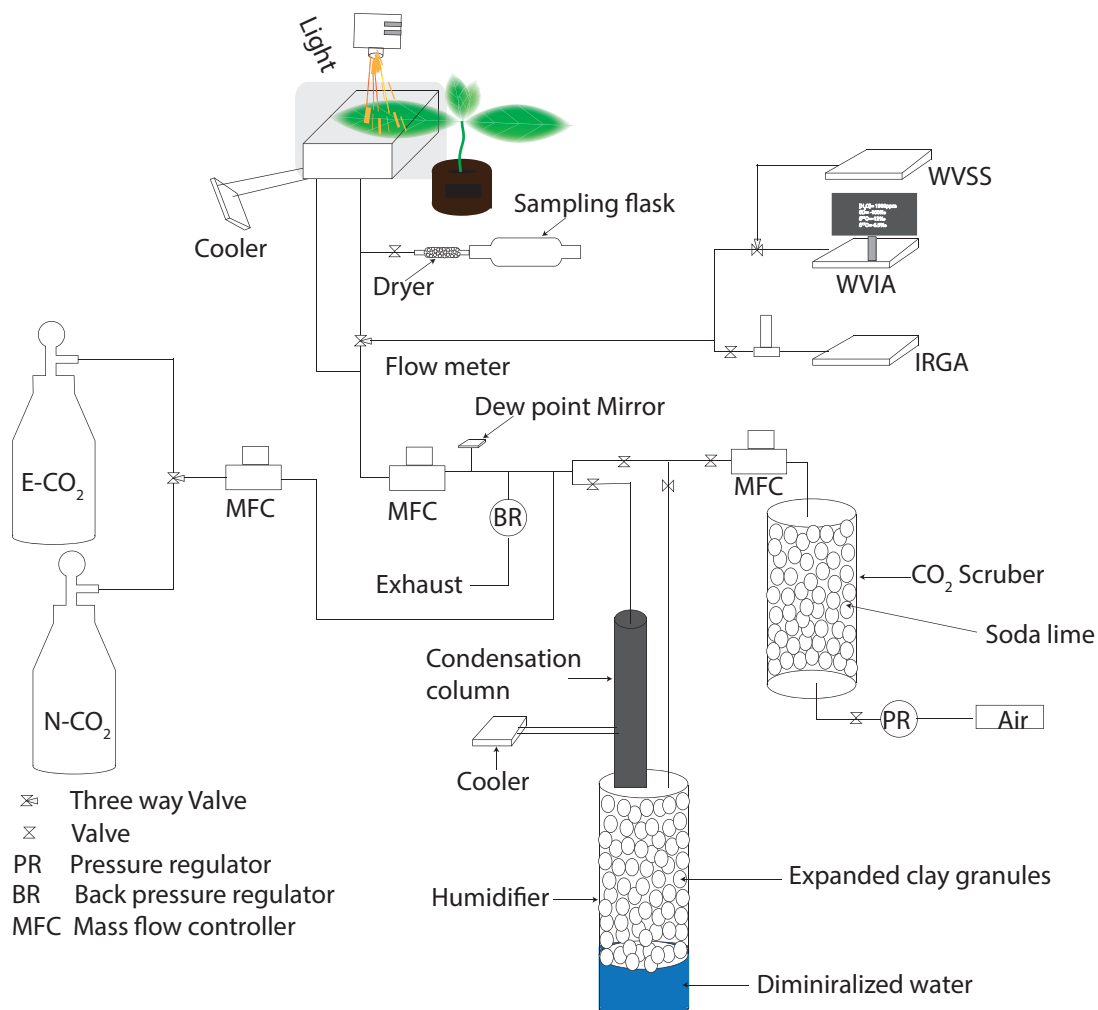


080 Figure 2 Illustration of the changes in $\Delta^{17}\text{O}$ for mixing of two different gases when the $\Delta^{17}\text{O}$ values are
calculated in logarithmic form, as a function of the fraction of CO_2 gas b . The blue and black circles show
the $\Delta^{17}\text{O}$ values of the mixing end members and the different colors show mixing lines for differences in
 $\delta^{18}\text{O}$.

085

090

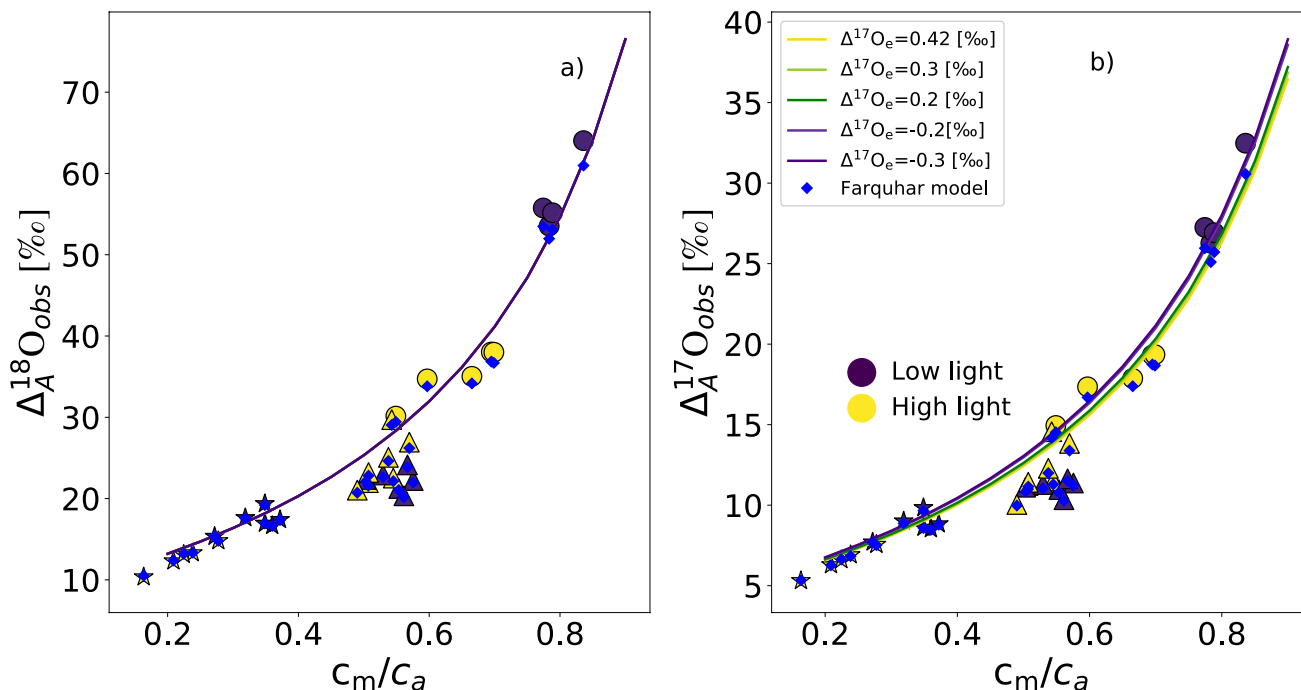
095



100

Figure 3 Schematic diagram of the leaf cuvette experimental setup. IRGA stands for the infrared gas analyzer, WVSS is the water vapor standard source, WVIA is the water vapor isotope analyzer, N-CO₂ is normal CO₂, E-CO₂ is ¹⁷O-enriched CO₂.

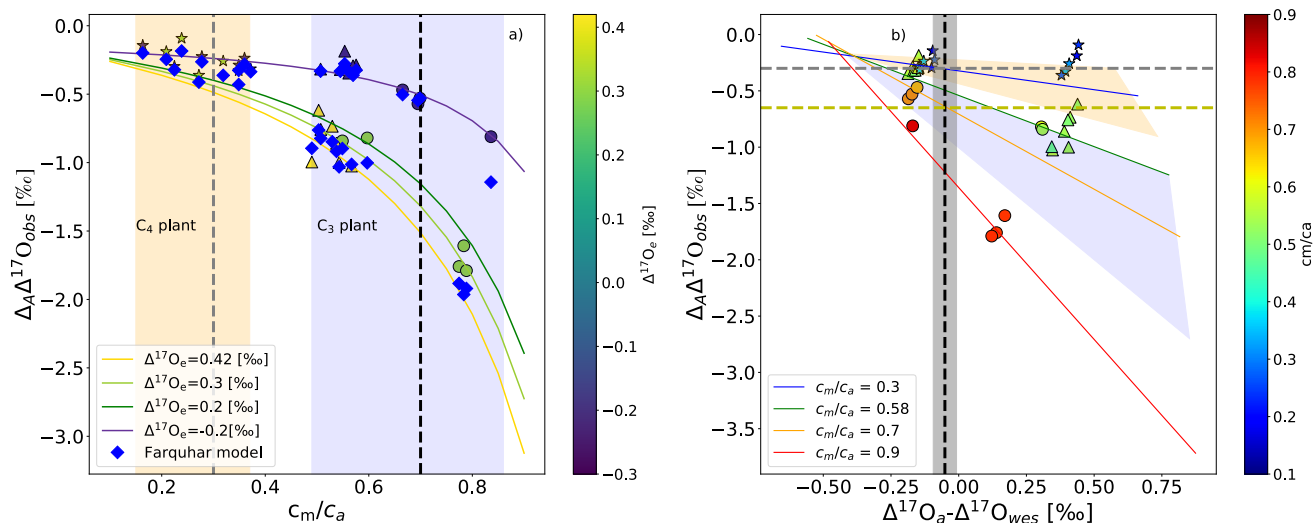
105



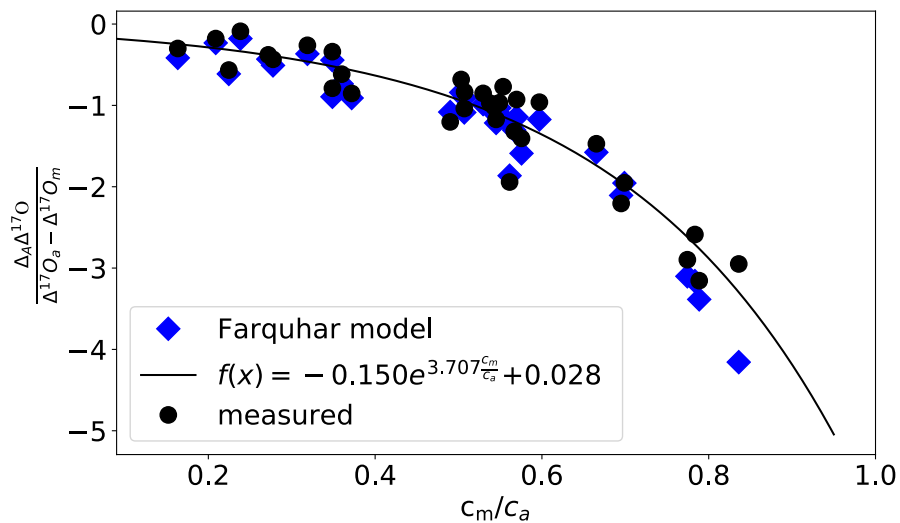
110 Figure 4 a) $\Delta_A^{18}\text{O}_{\text{obs}}$ and b) $\Delta_A^{17}\text{O}_{\text{obs}}$ during photosynthesis for two C_3 plants, sunflower (circles) and ivy (triangles) and C_4 plant maize (stars) as a function of c_m/c_a . The solid lines show results from the leaf cuvette model, where $\delta^{18}\text{O}$ of the CO_2 entering the cuvette is 30.47‰ while the $\delta^{17}\text{O}_e$ of the CO_2 is varied based on the $\Delta^{17}\text{O}_e$ of the CO_2 . The blue diamond dots are results from Farquhar model (Equation S12 in the supplementary material for $\Delta_A^{17}\text{O}_{\text{FM}}$ and Equation 7 for $\Delta_A^{18}\text{O}_{\text{FM}}$).



115

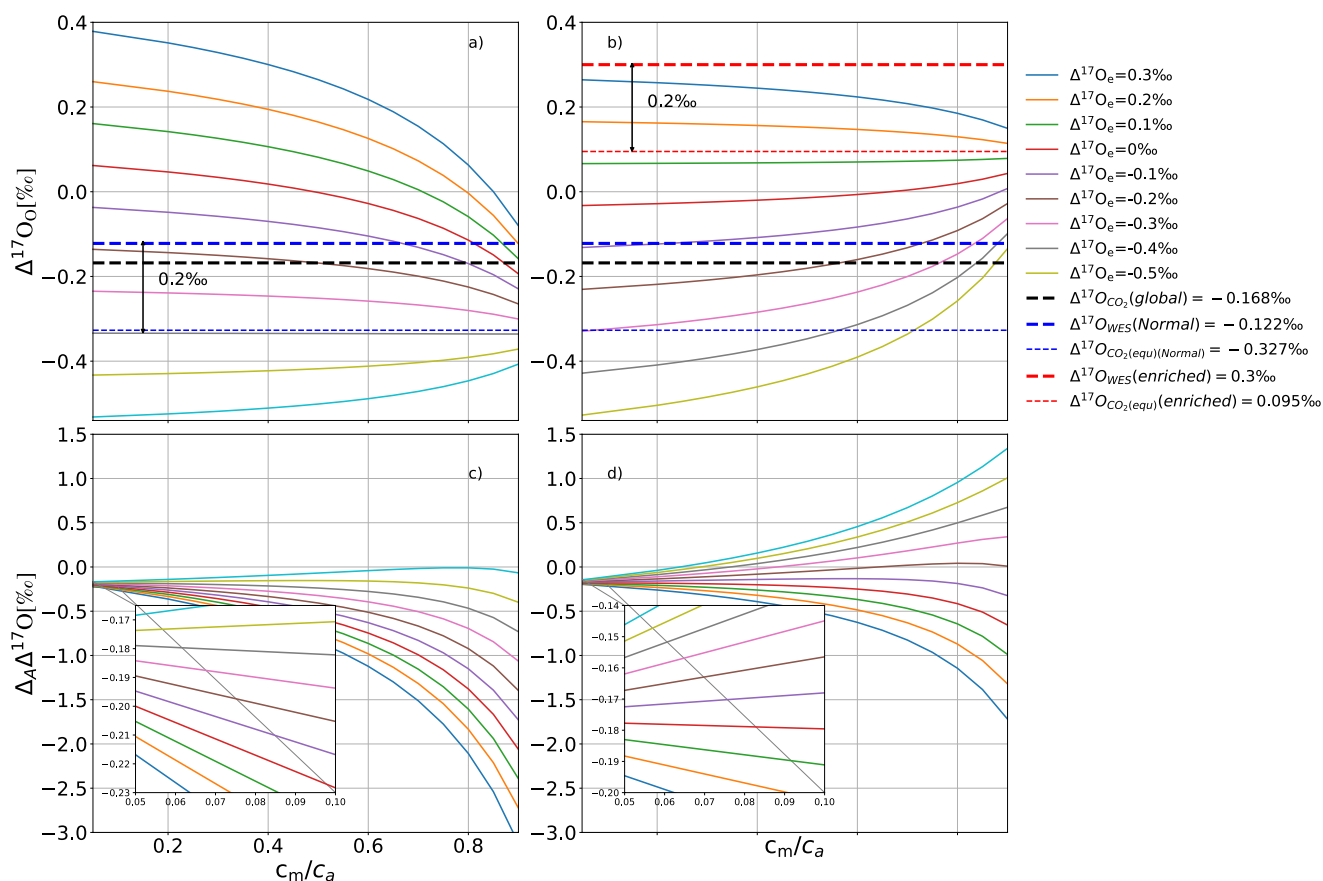


120 **Figure 5** a) $\Delta_A \Delta^{17}\text{O}$ of CO_2 as a function of c_m/c_a for isotopically different CO_2 gases entering the cuvette
 (color bar shows $\Delta^{17}\text{O}_e$) for sunflower (circles), ivy (triangles) and maize (stars). $\Delta_A \Delta^{17}\text{O}$ values calculated
 using the leaf cuvette model are shown as solid lines in corresponding colors ($\Delta^{17}\text{O}_e$ values given in the
 legend). The shaded areas indicate the c_m/c_a ranges for C_4 and C_3 plants and the vertical dashed lines
 indicate the mean c_m/c_a ratio used for extrapolating from the leaf scale to the global scale. The blue
 symbols represent results from the Farquhar model, calculated as $\Delta_A \Delta^{17}\text{O} = \ln(\Delta_A^{17}\text{O}_{\text{FM}}+1) - 0.528 \times \ln$
 125 $(\Delta_A^{18}\text{O}_{\text{FM}}+1)$. b) dependency of $\Delta_A \Delta^{17}\text{O}$ on the difference between the $\Delta^{17}\text{O}$ of CO_2 entering the cuvette
 and the $\Delta^{17}\text{O}$ of leaf water at the evaporation site color coded for different c_m/c_a ratios. The solid lines
 are results of the leaf cuvette model for different c_m/c_a ratios stated in the legend. The dashed vertical black
 line indicates the difference between the global average $\Delta^{17}\text{O}$ value for CO_2 (-0.168‰) and leaf water ($-$
 130 0.067‰) (Koren et al., 2019). The gray and yellow horizontal dashed lines indicate $\Delta_A \Delta^{17}\text{O}$ of C_4 and C_3
 plants for c_m/c_a ratio of 0.3 and 0.7, respectively globally.



135

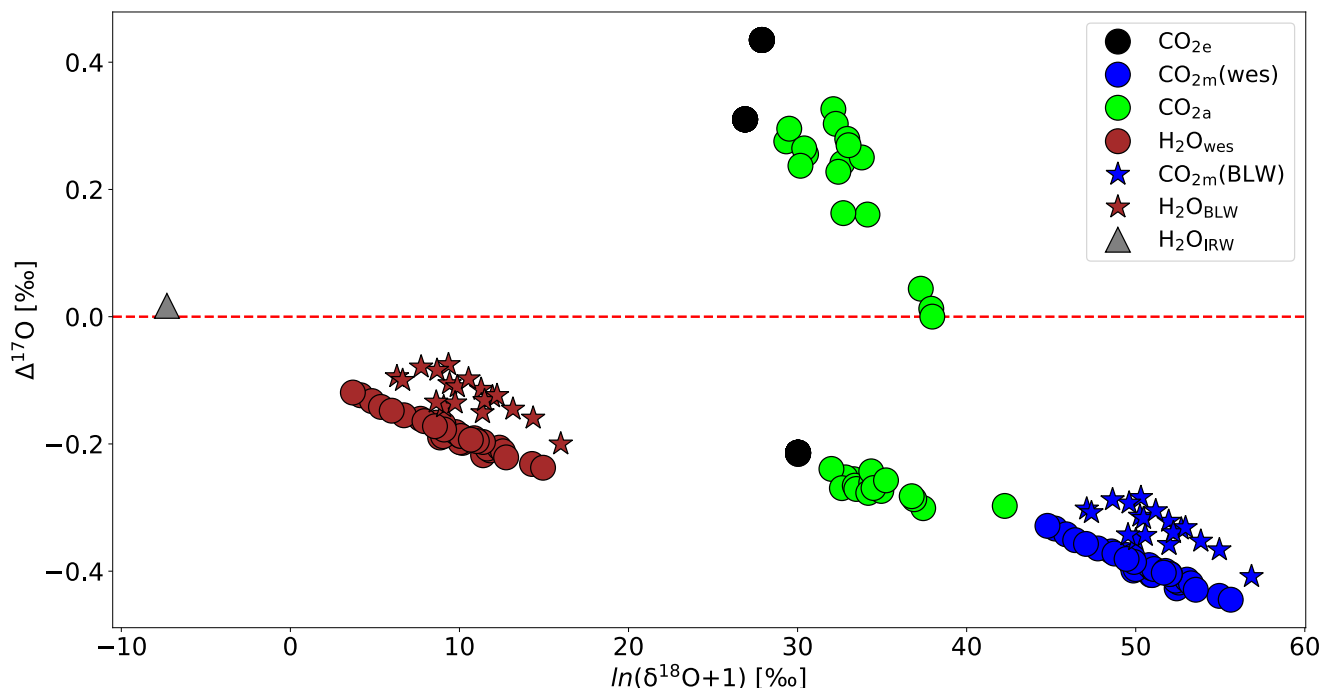
Figure 6 Dependency of $\Delta_A \Delta^{17}\text{O}$ on the relative difference on the $\Delta^{17}\text{O}$ CO_2 entering the leaf and the $\Delta^{17}\text{O}$ of CO_2 in equilibrium with leaf water against c_m/c_a ratio.



140

Figure 7 a) and b) $\Delta^{17}\text{O}_a$ as a function of c_m/c_a for various values of $\Delta^{17}\text{O}_e$ (see legend) for $\Delta^{17}\text{O}_{\text{wes}} = -0.122\text{‰}$ in a) and $\Delta^{17}\text{O}_{\text{wes}} = 0.300\text{‰}$ in b). c) and d) show the corresponding values for $\Delta_a\Delta^{17}\text{O}$. $\Delta^{17}\text{O}_{\text{global}}$ is the global average $\Delta^{17}\text{O}$ value for atmospheric CO_2 (Koren et al., 2019). When $\Delta^{17}\text{O}$ of CO_2 entering the cuvette is approximately 0.2‰ lower than the $\Delta^{17}\text{O}$ of leaf water at the $\text{CO}_2\text{-H}_2\text{O}$ exchange site, $\Delta^{17}\text{O}$ of the CO_2 leaving the cuvette does not change when c_m/c_a vary.

145



150 Figure 8 Isotopic composition of various relevant oxygen reservoirs that affect the $\Delta^{17}\text{O}$ of atmospheric CO_2 during photosynthesis: irrigation water (grey triangle), calculated leaf water at the evaporation site (brown circles), measured bulk leaf water (brown star), CO_2 entering the cuvette (black circles), CO_2 leaving the leaf cuvette (green circles), CO_2 equilibrated with leaf water at the evaporation site (blue circles), CO_2 equilibrated with bulk leaf water (blue stars).

155 Table 1: Summary for the parameters used of the extrapolation of leaf scale experiments to the global scale and the results obtained, and $\Delta^{17}\text{O}$ value of tropospheric CO_2 available measurements.

Parameters and values used for global estimation		
Parameter	Value	ref
GPP	120 PgCyr ⁻¹	(Beer et al., 2010)
f_{C4}	23%	(Still et al., 2003)
f_{C3}	77%	(Still et al., 2003)
c_m/c_a (C_3)	0.7	(Hoag et al., 2005)
c_m/c_a (C_4)	0.3	(Hoag et al., 2005)
$\Delta^{17}\text{O}$ leaf water (global mean, modelled)	$-0.067 \pm 0.04\text{‰}$	(Koren et al., 2019)
$\Delta^{17}\text{O}$ CO_2 (global mean, modelled)	$-0.168 \pm 0.013\text{‰}$	(Koren et al., 2019)
$\Delta_A \Delta^{17}\text{O}$ (global mean for C_4)	$-0.3 \pm 0.18\text{‰}$	(Figure 5b, for c_m/c_a ratio of 0.3)
$\Delta_A \Delta^{17}\text{O}$ (global mean for C_3)	$-0.65 \pm 0.18\text{‰}$	(Figure 5b, for c_m/c_a ratio of 0.7)
$\Delta_A \Delta^{17}\text{O}$ (global mean for whole vegetation)	$-0.57 \pm 0.14\text{‰}$	(Equation 13)



$\Delta_A \Delta^{17}\text{O}$ -isoflux (global mean for C ₄)	$-7.3 \pm 4\text{‰PgCyr}^{-1}$	(Equation 14, only for C ₄)
$\Delta_A \Delta^{17}\text{O}$ -isoflux (global mean for C ₃)	$-53 \pm 15\text{‰PgCyr}^{-1}$	(Equation 14, only for C ₃)
$\Delta_A \Delta^{17}\text{O}$ -isoflux (global mean for whole vegetation)	$-60 \pm 15\text{‰PgCyr}^{-1}$	(equation 14)
$\Delta_A \Delta^{17}\text{O}$ -isoflux (global mean for whole vegetation)	-47‰PgCyr^{-1}	(Hoag et al., 2005)
$\Delta_A \Delta^{17}\text{O}$ -isoflux (global mean for whole vegetation)	-42 to -92‰PgCyr^{-1}	(Hofmann et al., 2017)
$\Delta^{17}\text{O}$ value of tropospheric CO₂		
$\Delta^{17}\text{O}(\text{CO}_2)$ for CO ₂ samples collected in La Jolla-UCSD (California, USA) (1990 to 2000)	$-0.173 \pm 0.046\text{‰}$	(Thiemens et al., 2014)
$\Delta^{17}\text{O}(\text{CO}_2)$ for CO ₂ samples collected in Israel	$0.034 \pm 0.010\text{‰}$	(Barkan and Luz, 2012)
$\Delta^{17}\text{O}(\text{CO}_2)$ for CO ₂ samples collected in South china sea (2013-2014)	$-0.159 \pm 0.084\text{‰}$	(Liang et al., 2017a; Liang et al., 2017b)
$\Delta^{17}\text{O}(\text{CO}_2)$ for CO ₂ samples collected in Taiwan (2012-2015)	$-0.150 \pm 0.080\text{‰}$	(Liang et al., 2017a; Liang et al., 2017b)
$\Delta^{17}\text{O}(\text{CO}_2)$ for CO ₂ samples collected in California (USA) (2015)	$-0.177 \pm 0.029\text{‰}$	(Liang et al., 2017a; Liang et al., 2017b)
$\Delta^{17}\text{O}(\text{CO}_2)$ for CO ₂ samples collected in Göttingen (Germany) (2010-2012)	$-0.122 \pm 0.065\text{‰}$	(Hofmann et al., 2017)